Flavor and new physics opportunities with rare charm decays into leptons

Stefan de Boer and Gudrun Hiller

Phys. Rev. D **93**, 074001 — Published 1 April 2016

DOI: 10.1103/PhysRevD.93.074001

Flavor & new physics opportunities with rare charm decays into leptons

Stefan de Boer* and Gudrun Hiller†
Fakultät für Physik, TU Dortmund, Otto-Hahn-Str.4, D-44221 Dortmund, Germany

Updated standard model predictions for $D_{(s)} \to P l^+ l^-$, $l = e, \mu$, $P = \pi, K$ and inclusive decays are presented. Model-independent constraints on $|\Delta C| = |\Delta U| = 1$ Wilson coefficients are worked out. New physics (NP) opportunities arise in semileptonic branching ratios for very large couplings only, however, are not excluded outside the resonance regions yet. The NP potential of resonance-assisted CP-asymmetries and angular observables is worked out. Predictions are given for leptoquark models, and include lepton flavor violating and dineutrino decays. Whether NP can be seen depends on flavor patterns, and vice versa.

I. INTRODUCTION

The study of flavor-changing neutral current (FCNC) transitions is a key tool to explore the generational structure of standard model (SM) fermions and to look for physics beyond the standard model (BSM). While analyses involving b-quarks are matured to precision level [1], the investigation of charm FCNCs is much less advanced, as corresponding rates are highly GIM-suppressed and experimentally challenging and/or decay modes subjected to resonance contributions, shielding the electroweak physics.

Semileptonic charm hadron decays provide an opportunity to probe for new physics in $|\Delta C| = |\Delta U| = 1$ FCNCs [2]. Such processes, induced by $c \to u l^+ l^-$, $l = e, \mu$, allow to kinematically reduce the resonance background via $c \to Mu \to l^+ l^- u$, where M denotes a meson with mass m_M decaying to dileptons such as $M = \eta^{(\prime)}, \rho, \omega, \phi$, by kinematic cuts in the dilepton invariant mass squared q^2, notably $q^2 \gtrsim m_\phi^2$. The available phase space is, however, limited, at most $\Delta q^2 \sim 2\,\mathrm{GeV}^2$ for the most favorable decays $D^+ \to \pi^+ l^+ l^-$, and the resonance tails remain overwhelming in the decay rates until the endpoint. To access short-distance physics becomes still possible in two situations: *i)* The BSM-induced rates are much larger than the SM background. *ii)* Using SM null tests, that is, specifically chosen observables. The latter are generically related to SM (approximate) symmetries, such as CP in $c \to u$ transitions, and include various ratios and asymmetries.

In this work we pursue the analysis of rare charm observables using CP-asymmetries and those related to leptons, lepton flavor violating (LFV) decays $c \to u e^\pm \mu^\mp$. The latter have essentially no SM contribution due to the smallness of neutrino masses. Importantly, there are no photon-induced dilepton effects, the usual source of resonance pollution. Therefore, for LFV charm decays no cuts in q^2 are required from the theory perspective. Similarly $c \to u \nu \bar{\nu}$ processes have essentially zero SM background and factorize in the full region of q^2. In addition, the study of rare charm decays has great prospects at the LHCb and Belle II experiments, as well as BES III [3], and possible other future high luminosity flavor facilities [4, 5].

Leptoquarks are particularly interesting for flavor physics because they link quark to lepton flavor. A rich phenomenology and correlations between different kinds of flavor transitions, K-, D- and B-decays as well as LFV, allow to probe the SM and flavor models simultaneously. Naturally, CP-violation, lepton-nonuniversality (LNU) and LFV arise. We work out correlations in a number of flavor benchmarks for scalar and vector leptoquarks that induce $c \to u l^+ l^-$. Some of these are currently discussed in the context of B-physics anomalies hinting LNU [6–10].

The plan of the paper is as follows: In Sec. II we work out SM predictions for $c \to u l^+ l^-$ processes, including recent results for higher order perturbative contributions [11]. We identify BSM windows in rare exclusive $c \to u l^+ l^-$ modes. In Sec. III constraints and predictions are worked out model-independently and within leptoquark scenarios, amended by flavor patterns. In Sec. IV we summarize. Auxiliary information is compiled in several appendices.

II. STANDARD MODEL PREDICTIONS

We work out SM predictions for exclusive semileptonic charm decays. In Sec. II A we obtain (N)NLO results for the (effective) $|\Delta C| = |\Delta U| = 1$ coefficients. In Sec. II B we work out branching ratios, including resonance effects

*Electronic address: stefan.deboer@tu-dortmund.de
†Electronic address: ghiller@physik.uni-dortmund.de

and compare to data.

A. Wilson Coefficients

We write the $c \to u l^+ l^-$ effective weak Lagrangian [11–13] with two-step matching at the W-mass scale and the b-quark mass scale, respectively, as

$$\mathcal{L}_{\text{eff}}^{\text{weak}}\big|_{m_W \geq \mu > m_b} = \frac{4G_F}{\sqrt{2}} \sum_{q=d,s,b} V_{cq}^* V_{uq} \left(\tilde{C}_1(\mu) P_1^{(q)}(\mu) + \tilde{C}_2(\mu) P_2^{(q)}(\mu) \right) , \tag{1}$$

$$\mathcal{L}_{\text{eff}}^{\text{weak}}\big|_{m_b > \mu \geq m_c} = \frac{4G_F}{\sqrt{2}} \sum_{q=d,s} V_{cq}^* V_{uq} \left(\tilde{C}_1(\mu) P_1^{(q)}(\mu) + \tilde{C}_2(\mu) P_2^{(q)}(\mu) + \sum_{i=3}^{10} \tilde{C}_i(\mu) P_i(\mu) \right) . \tag{2}$$

Here, G_F is the Fermi constant and V_{ij} denote the Cabibbo–Kobayashi–Maskawa (CKM) matrix elements. Within the OPE (1), (2) heavy fields are integrated in the Wilson coefficients $\tilde{C}_i$ and the operators P_i are composed out of light fields. The SM operators up to dimension six read [14–16]

$$P_1^{(q)} = (\bar{u}_L \gamma_{\mu_1} T^a q_L)(\bar{q}_L \gamma^{\mu_1} T^a c_L) , \tag{3}$$

$$P_2^{(q)} = (\bar{u}_L \gamma_{\mu_1} q_L)(\bar{q}_L \gamma^{\mu_1} c_L) , \tag{4}$$

$$P_3 = (\bar{u}_L \gamma_{\mu_1} c_L) \sum_{\{q: m_q < \mu\}} (\bar{q} \gamma^{\mu_1} q) , \tag{5}$$

$$P_4 = (\bar{u}_L \gamma_{\mu_1} T^a c_L) \sum_{\{q: m_q < \mu\}} (\bar{q} \gamma^{\mu_1} T^a q) , \tag{6}$$

$$P_5 = (\bar{u}_L \gamma_{\mu_1} \gamma_{\mu_2} \gamma_{\mu_3} c_L) \sum_{\{q: m_q < \mu\}} (\bar{q} \gamma^{\mu_1} \gamma^{\mu_2} \gamma^{\mu_3} q) , \tag{7}$$

$$P_6 = (\bar{u}_L \gamma_{\mu_1} \gamma_{\mu_2} \gamma_{\mu_3} T^a c_L) \sum_{\{q: m_q < \mu\}} (\bar{q} \gamma^{\mu_1} \gamma^{\mu_2} \gamma^{\mu_3} T^a q) , \tag{8}$$

$$P_7 = \frac{e}{g_s^2} m_c \, (\bar{u}_L \sigma^{\mu_1 \mu_2} c_R) \, F_{\mu_1 \mu_2} , \tag{9}$$

$$P_8 = \frac{1}{g_s} m_c \, (\bar{u}_L \sigma^{\mu_1 \mu_2} T^a c_R) \, G^a_{\mu_1 \mu_2} , \tag{10}$$

$$P_9 = \frac{e^2}{g_s^2} (\bar{u}_L \gamma_{\mu_1} c_L) \left(\bar{l} \gamma^{\mu_1} l \right) , \tag{11}$$

$$P_{10} = \frac{e^2}{g_s^2} (\bar{u}_L \gamma_{\mu_1} c_L) \left(\bar{l} \gamma^{\mu_1} \gamma_5 l \right) , \tag{12}$$

where $q_{L,R} = (1 \mp \gamma_5)/2 \, q$ denotes chiral quark fields, T^a are the $SU(3)_C$ generators, e is the electromagnetic coupling, g_s is the strong coupling, $\sigma^{\mu_1 \mu_2} = i[\gamma^{\mu_1}, \gamma^{\mu_2}]/2$, $F_{\mu_1 \mu_2}$ is the electromagnetic field strength tensor and $G^a_{\mu_1 \mu_2}$ is the chromomagnetic field strength tensor.

In this section we give results for the (Next-to-)Next-to-Leading-Order (N)NLO QCD SM Wilson coefficients

$$\tilde{C}_i(\mu) = \tilde{C}_i^{(0)}(\mu) + \frac{\alpha_s(\mu)}{4\pi} \tilde{C}_i^{(1)}(\mu) + \left(\frac{\alpha_s(\mu)}{4\pi} \right)^2 \tilde{C}_i^{(2)}(\mu) + \mathcal{O}\left(\alpha_s^3(\mu) \right) . \tag{13}$$

$\tilde{C}_{1,2}(\mu_W)$ can be inferred from [15, 17] and $\tilde{C}_{3-10}(\mu_W) = 0$ due to CKM unitarity for vanishing light quark masses. If one were to keep finite light quark masses in the Wilson coefficients at μ_W as in [18–20] spurious large logarithms are induced, *e.g.*, [21]

$$\sum_{q=d,s,b} V_{cq}^* V_{uq} \tilde{C}_9^{(q)}(\mu_W) \simeq V_{cs}^* V_{us} \frac{(-2)}{9} \ln \frac{m_s^2}{m_d^2} \simeq -0.29 , \tag{14}$$

a procedure that is not consistent with the factorization of scales in the effective Lagrangian [11, 13]. Logarithms are resummed to all orders in perturbation theory via the renormalization group (RG) equation [17, 22, 23]. After

RG-evolution of $\tilde{C}_{1,2}$ from μ_W to μ_b, we integrate out the b-quark at μ_b, which induces non-zero contributions to P_{3-10}, and then RG-evolve $\tilde{C}_{1-10}$ from μ_b to μ_c. The resummation to NNLO is worked out in [11], to which we refer for details on the RG equation, anomalous dimensions and matching. The results of this NNLO evolution are included in the numerical analysis in this work. Using the parameters compiled in App. A we find the SM Wilson coefficients at the charm quark mass given in Table I.

	$j=1$	$j=2$	$j=3$	$j=4$	$j=5$	$j=6$	$j=7$	$j=8$	$j=9$	$j=10$
$\tilde{C}_j^{(0)}$	-1.0275	1.0926	-0.0036	-0.0604	0.0004	0.0007	0	0	-0.0030	0
$(\alpha_s/(4\pi))\,\tilde{C}_j^{(1)}$	0.3214	-0.0549	-0.0025	-0.0312	0.0000	-0.0002	0.0035	-0.0020	-0.0064	0
$(\alpha_s/(4\pi))^2\,\tilde{C}_j^{(2)}$	0.0766	-0.0037	-0.0019	-0.0008	0.0001	0.0003	0.0002	-0.0003	-0.0037	0
$\tilde{C}_j$	-0.6295	1.0339	-0.0080	-0.0924	0.0005	0.0008	0.0037	-0.0023	-0.0131	0

TABLE I: The ith order contributions $(\alpha_s/(4\pi))^i\,\tilde{C}_j^{(i)}$, $i=0,1,2$ to the SM Wilson coefficients, see Eq. (13), at $\mu_c = m_c$. The last row gives their sum, $\tilde{C}_j(m_c)$.

We write the matrix elements of the operators $P_{1-6,8}$ in terms of effective Wilson coefficients $C_{7,9}^{\rm eff}(\mu_c)$ and $C_{10}^{\rm eff}(\mu_c) = 0$. We find to one-loop order

$$\begin{aligned} C_9^{\mathrm{eff}(q)}(q^2) = \tilde{C}_9 + \frac{\alpha_s}{4\pi}\Big[& \frac{8}{27}\tilde{C}_1 + \frac{2}{9}\tilde{C}_2 - \frac{8}{9}\tilde{C}_3 - \frac{32}{27}\tilde{C}_4 - \frac{128}{9}\tilde{C}_5 - \frac{512}{27}\tilde{C}_6 \\ & + L(m_c^2,q^2)\left(\frac{28}{9}\tilde{C}_3 + \frac{16}{27}\tilde{C}_4 + \frac{304}{9}\tilde{C}_5 + \frac{256}{27}\tilde{C}_6\right) \\ & + L(m_s^2,q^2)\left(-\frac{4}{3}\tilde{C}_3 - \frac{40}{3}\tilde{C}_5\right) \\ & + L(0,q^2)\left(\frac{16}{9}\tilde{C}_3 + \frac{16}{27}\tilde{C}_4 + \frac{184}{9}\tilde{C}_5 + \frac{256}{27}\tilde{C}_6\right) \\ & + \left(\delta_{qs}L(m_s^2,q^2) + \delta_{qd}L(0,q^2)\right)\left(-\frac{8}{27}\tilde{C}_1 - \frac{2}{9}\tilde{C}_2\right)\Big] \\ & + \left(\frac{\alpha_s}{4\pi}\right)^2 F_8^{(9)}(q^2/m_c^2)C_8^{\rm eff}\,, \end{aligned} \tag{15}$$

in agreement with the corresponding calculation in b-quark decays [24] and

$$C_7^{\mathrm{eff}(q)}(q^2) = \tilde{C}_7 + \frac{\alpha_s}{4\pi}\sum_{i=1}^{6} y_i^{(7)}\tilde{C}_i + \left(\frac{\alpha_s}{4\pi}\right)^2\left[\left(-\frac{1}{6}\tilde{C}_1^{(0)} + \tilde{C}_2^{(0)}\right) f(m_q^2/m_c^2) + F_8^{(7)}(q^2/m_c^2)C_8^{\rm eff}\right] \tag{16}$$

with $C_8^{\rm eff} = \tilde{C}_8^{(1)} + \sum_{i=1}^{6} y_i^{(8)}\tilde{C}_i^{(0)}$ and $\tilde{C}_{1-6}$ consistently expanded to order α_s. The functions f, L and $F_8^{(7,9)}$ and the coefficients $y_i^{(7,8)}$ are given in App. B. The coefficients $C_{7,9}^{\rm eff} \sim V_{cb}^* V_{ub}$ induced by the two-loop matrix elements of P_{3-6} and $C_9^{\rm eff}$ induced by the two-loop matrix elements of $P_{1,2}$ are not known presently and neglected in the following analysis. Hence, the NNLO result is not complete and labeled as (N)NLO.

For the phenomenological analyses in Secs. II B and III it is customary to redefine the dilepton and electromagnetic dipole operators and use

$$Q_7 = \frac{m_c}{e}(\bar{u}\sigma^{\mu\nu}P_R c)F_{\mu\nu}\,, \tag{17}$$

$$Q_9 = (\bar{u}\gamma_\mu P_L c)\left(\bar{l}\gamma^\mu l\right)\,, \tag{18}$$

$$Q_{10} = (\bar{u}\gamma_\mu P_L c)\left(\bar{l}\gamma^\mu\gamma_5 l\right)\,. \tag{19}$$

Their effective coefficients $C_{7,9,10} = C_{7,9,10}(q^2)$ are related to the ones of $P_{7,9,10}$ as

$$C_{7,9,10}(\mu_c) = \frac{4\pi}{\alpha_s(\mu_c)}\left[V_{cd}^* V_{ud} C_{7,9,10}^{\mathrm{eff}(d)}(\mu_c) + V_{cs}^* V_{us} C_{7,9,10}^{\mathrm{eff}(s)}(\mu_c)\right]\,. \tag{20}$$

Using $\sum_{q=d,s,b} V_{cq}^* V_{uq} = 0$ makes manifest that the coefficients are GIM or Cabibbo suppressed, specifically, $L(m_s^2,q^2) - L(0,q^2) = \mathcal{O}(m_s^2/m_c^2)$ at high q^2.

The effective coefficient C_9, Eq. (20), in the SM is shown in Fig. 1. C_7 is not shown because its q^2-dependence is negligible. Note that $C_{10} = 0$, and that C_7 and C_9 are primarily set by the matrix elements of $P_{1,2}$. For $\mu_c = m_c$, $C_7 \simeq (-0.0011 - 0.0041i)$ and $C_9 \simeq -0.021 X_{ds}$, where $X_{ds} = (V_{cd}^* V_{ud} L(m_d^2, q^2) + V_{cs}^* V_{us} L(m_s^2, q^2))$. Varying $m_c/\sqrt{2} \leq \mu_c \leq \sqrt{2} m_c$ we find $(-0.0014 - 0.0054i) \leq C_7 \leq (-0.00087 - 0.0033i)$ and $-0.060 X_{ds}(\mu_c = \sqrt{2} m_c) \leq C_9 \leq 0.030 X_{ds}(\mu_c = m_c/\sqrt{2})$. For $q^2 \gtrsim 1\,\mathrm{GeV}^2$, we obtain as a result a small SM contribution, $|C_9| \lesssim 5 \cdot 10^{-4}$.

The one-loop contribution to C_9 is suppressed by cancellations between $\tilde{C}_1$ and $\tilde{C}_2$. Therefore, the two-loop matrix element of $P_{1,2}^{(q)}(\mu_c)$, $q = d, s$ inducing C_9, of the order $|V_{cd}^* V_{ud}| \times \alpha_s(\mu_c)/(4\pi) \times$GIM-type m_s^2/m_c^2-suppression at $q^2 = \mathcal{O}(m_c^2)$[1], could numerically be of similar size as the (N)NLO one.

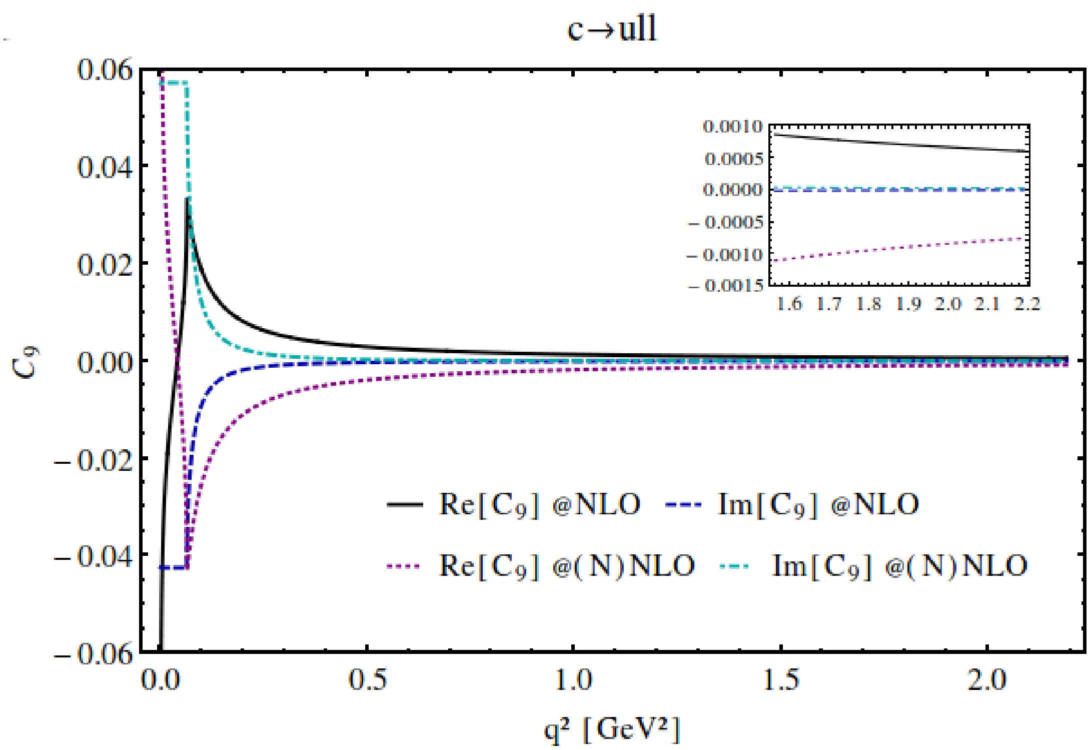

FIG. 1: The effective coefficient $C_9(\mu_c = m_c)$ given in Eq. (20) at NLO and the pure (N)NLO-terms in the SM. The two-loop matrix elements of $P_{1,2}$ are not known presently and not included. See text for details.

B. Phenomenology

In this section we study the SM phenomenology of $D^+ \to \pi^+ \mu^+ \mu^-$ decays and introduce SM null tests. Decay distributions are given in App. D, and the requisite form factors f_i are defined in App. C. In particular, in our numerical analysis the vector/axialvector form factor f_+ is taken from data [26], and the dipole one f_T is related to f_+ through the (improved) Isgur-Wise relations at low and high q^2, between which we interpolate, *cf.* App. C. A third form factor, f_0, does not contribute at short distances as it multiplies C_{10}, which vanishes in the SM. $f_+(q^2)$, $f_T(q^2)$ and $f_0(q^2)$, which can contribute in SM extensions, can be seen in Fig. 5. In our calculation we expand squared amplitudes to order α_s^2 and apply the pole mass for m_c in matrix elements.

Integrating the distribution in different q^2-bins yields the non-resonant SM branching ratios given in Table II. The first uncertainty given corresponds to the normalization, which is dominated by the D-lifetime, relative to which CKM uncertainties are subdominant. The dominant theory uncertainty stems from the charm scale μ_c, which here is varied within $m_c/\sqrt{2} \leq \mu_c \leq \sqrt{2} m_c$. The effect of a larger upper limit on μ_c is to enhance (decrease) the branching ratios at low (high) q^2. For instance, allowing for values of μ_c as large as 4 GeV doubles (cuts into halves) the branching ratios

---

[1] This behavior is also supported by a related calculation in $b \to sll$ decays [25].

obtained for $\mu_c = \sqrt{2}m_c$ at low (high) q^2. Consequently, the effect on the full q^2-range of integration averages out. The other scales are varied within $m_{W,b}/2 \le \mu_{W,b} \le 2m_{W,b}$. Uncertainties due to power corrections are not included. Electroweak corrections, which are subleading relative to QCD-ones, are neglected. We checked this explicitly by calculating the effects of electromagnetic mixing among the P_i at leading order [27, 28]. Additional uncertainties from $\alpha_s(m_Z) = 0.1185 \pm 0.0006$ amount to a few percent.

Further non-resonant SM branching fractions for inclusive $c \to ull$ decays and additional $D \to Pll$ decays are also worked out and given in App. E. Our findings are consistent with [13, 29], but disagree with those of [18–20] by orders of magnitude. As already discussed around Eq. (14), this goes back to the inclusion of light quark masses in [18–20] in the matching at μ_W.

q^2-bin	$\mathcal{B}(D^+ \to \pi^+\mu^+\mu^-)^{\rm SM}_{\rm nr}$	90% CL limit [30]
full q^2: $(2m_\mu)^2 \le q^2 \le (m_{D^+} - m_{\pi^+})^2$	$3.7 \cdot 10^{-12}\,(\pm1, \pm3, ^{+16}_{-15}, \pm1, ^{+3}_{-1}, ^{+158}_{-1}, ^{+16}_{-12})$	$7.3 \cdot 10^{-8}$
low q^2: $0.250^2\,\mathrm{GeV}^2 \le q^2 \le 0.525^2\,\mathrm{GeV}^2$	$7.4 \cdot 10^{-13}\,(\pm1, \pm4, ^{+23}_{-21}, ^{+10}_{-11}, ^{+10}_{-1}, ^{+238}_{-23}, ^{+6}_{-5})$	$2.0 \cdot 10^{-8}$
high q^2: $q^2 \ge 1.25^2\,\mathrm{GeV}^2$	$7.4 \cdot 10^{-13}\,(\pm1, \pm6, ^{+15}_{-14}, \pm6, ^{+0}_{-1}, ^{+136}_{-45}, ^{+27}_{-20})$	$2.6 \cdot 10^{-8}$

TABLE II: Non-resonant SM branching fractions of $D^+ \to \pi^+\mu^+\mu^-$ decays normalized to the total width. Non-negligible uncertainties correspond to (normalization, m_c, m_s, μ_W, μ_b, μ_c, f_+), respectively, and are given in percent. In the last column we give the corresponding experimental 90% CL upper limits [30].

Next we model the contributions from resonances by using a (constant width) Breit-Wigner shape for $C_9 \to C_9^{\rm R}$ for vector and $C_P \to C_P^{\rm R}$ for pseudoscalar mesons

$$
\begin{aligned}
C_9^{\rm R} &= a_\rho e^{i\delta_\rho}\left(\frac{1}{q^2 - m_\rho^2 + i m_\rho \Gamma_\rho} - \frac{1}{3}\frac{1}{q^2 - m_\omega^2 + i m_\omega \Gamma_\omega}\right) + \frac{a_\phi e^{i\delta_\phi}}{q^2 - m_\phi^2 + i m_\phi \Gamma_\phi}\,, \\
C_P^{\rm R} &= \frac{a_\eta e^{i\delta_\eta}}{q^2 - m_\eta^2 + i m_\eta \Gamma_\eta} + \frac{a_{\eta'}}{q^2 - m_{\eta'}^2 + i m_{\eta'} \Gamma_{\eta'}}\,,
\end{aligned}
\tag{21}
$$

where Γ_M denotes the total width of resonance $M = \eta^{(\prime)}, \rho, \omega, \phi$ and we safely neglected the SM's CP-violating effects. Since the branching fraction of $D^+ \to \pi^+\omega$ decays is not measured yet, and also to reduce the number of parameters, one can use isospin to relate it to the one of the decay $D^+ \to \pi^+\rho$ [29]. While there are clearly corrections to this ansatz for the ω, these are subdominant relative to the dominant contributions from the ρ due to its large width.

Approximating $\mathcal{B}(D^+ \to \pi^+ M(\to \mu^+\mu^-)) \simeq \mathcal{B}(D^+ \to M\pi^+)\mathcal{B}(M \to \mu^+\mu^-)$ and taking the right-hand side from data [31] and $\mathcal{B}(\eta' \to \mu^+\mu^-) \sim \mathcal{O}(10^{-7})$ [31, 32], we obtain

$$
\begin{aligned}
a_\phi &= 0.24^{+0.05}_{-0.06}\,\mathrm{GeV}^2\,, \quad a_\rho = 0.17 \pm 0.02\,\mathrm{GeV}^2\,, \\
a_\eta &= 0.00060^{+0.00004}_{-0.00005}\,\mathrm{GeV}^2\,, \quad a_{\eta'} \sim 0.0007\,\mathrm{GeV}^2\,.
\end{aligned}
\tag{22}
$$

We note that the present experimental upper limit on $\mathcal{B}(D^+ \to \omega\pi^+)$ yields $a_\omega \lesssim 0.04$, somewhat below the isospin prediction, $a_\rho/3$.

The SM differential branching fraction of $D^+ \to \pi^+\mu^+\mu^-$ decays is shown in Fig. 2. The dominant resonance contributions above the ϕ-peak are due to the ϕ and the ρ. The relative strong phases $\delta_{\phi,\rho,\eta}$ are varied independently within $-\pi$ and π. The dominant uncertainty stems from the unknown phases, only near the resonance peaks the uncertainties in the factors a_M become noticeable. At high q^2 the resonances die out with increasing q^2, however slowly. For instance, we obtain $|C_9^{\rm R}(1.5\,\mathrm{GeV}^2)| \lesssim 0.8$ and $|C_9^{\rm R}(2\,\mathrm{GeV}^2)| \lesssim 0.4$, exceeding by many orders of magnitude the SM short-distance contribution to Q_9.

We learn the following: There is room for new physics below the current search limits [30] and above the resonance contribution; at very high, and very low q^2. In either case it will require large BSM contributions to the Wilson coefficients to be above the resonant background. We will quantify this in Sec. III.

The dominance of resonances in the decay rate for SM-like Wilson coefficients is common to all $c \to ul^+l^-$ induced processes, such as inclusive $D \to X_u l^+l^-$, or other exclusive decays, *e.g.*, $D \to \pi\pi l^+l^-$ [33] and $\Lambda_c \to pl^+l^-$. Choosing $c \to ul^+l^-$ induced decay modes other than $D^+ \to \pi^+l^+l^-$ does not help gaining BSM sensitivity in the dilepton spectrum, however, other modes may allow to construct more advantageous observables. Here we discuss opportunities in semileptonic exclusive decays with observables where the resonance contribution is not obstructing SM tests.

Clean SM tests are provided by the angular distribution in $D \to \pi l^+l^-$ decays, notably, the lepton forward-backward asymmetry $A_{\rm FB}$ and the "flat" term [34], F_H, see App. D. Both observables are null tests of the SM and require scalar/pseudoscalar operators and tensors to be non-negligible. A promising avenue to probe operators with

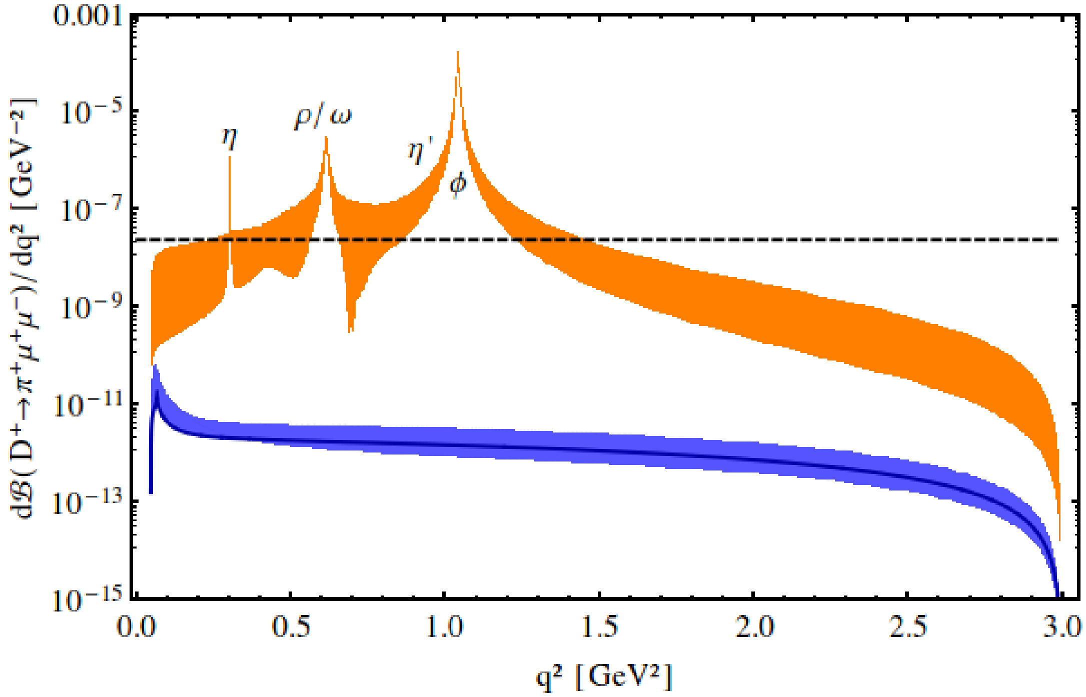

FIG. 2: The differential branching fraction $\mathrm{d}\mathcal{B}(D^+ \to \pi^+\mu^+\mu^-)/\mathrm{d}q^2$ in the SM. The solid blue curve is the non-resonant prediction at $\mu_c = m_c$ and the lighter blue band its μ_c-uncertainty. The orange band is the pure resonant contribution taking into account the uncertainties specified in Eq. (22) at 1 σ and varying the relative strong phases. The dashed black line denotes the 90% CL experimental upper limit [30].

Lorentz structures closer to the ones present in the SM is to study CP-asymmetries in the rate

$$A_{CP}(q^2) = \frac{\mathrm{d}\Gamma/\mathrm{d}q^2 - \mathrm{d}\bar{\Gamma}/\mathrm{d}q^2}{\int_{q^2_{\rm min}}^{q^2_{\rm max}} \mathrm{d}q^2 (\mathrm{d}\Gamma/\mathrm{d}q^2 + \mathrm{d}\bar{\Gamma}/\mathrm{d}q^2)}\,, \tag{23}$$

where $\mathrm{d}\bar{\Gamma}/\mathrm{d}q^2$ denotes the differential decay rate of the CP-conjugated mode, $D^- \to \pi^- l^+ l^-$. The difference of the widths can be written as

$$\begin{aligned}\frac{\mathrm{d}\Gamma}{\mathrm{d}q^2} - \frac{\mathrm{d}\bar{\Gamma}}{\mathrm{d}q^2} &= -\frac{G_F^2 \alpha_e^2}{384\pi^5 m_D^3}\sqrt{\lambda^3(m_D^2, m_P^2, q^2)\left(1 - 4\frac{m_l^2}{q^2}\right)}\left(1 + 2\frac{m_l^2}{q^2}\right) \\ &\times \left(\mathrm{Im}[V_{cd}^* V_{ud}(V_{cs} V_{us}^*)]\mathrm{Im}[c_d c_s^*] + \mathrm{Im}[V_{cd}^* V_{ud}\Delta_9^*]\mathrm{Im}[c_d] f_+ + \mathrm{Im}[V_{cs}^* V_{us}\Delta_9^*]\mathrm{Im}[c_s] f_+\right)\,,\end{aligned} \tag{24}$$

where the first term in the last row corresponds to the tiny SM prediction whereas the ones driven by $\Delta_9 = C_9^{BSM} + C_9'$ correspond to possible BSM contributions, and

$$c_d = \frac{4\pi}{\alpha_s} 2 C_7^{\mathrm{eff}(d)} f_T \frac{m_c}{m_D} + C_9^{\mathrm{R}}|_{\rho-only}\frac{f_+}{V_{cd}^* V_{ud}}\,, \tag{25}$$

$$c_s = \frac{4\pi}{\alpha_s} 2 C_7^{\mathrm{eff}(s)} f_T \frac{m_c}{m_D} + C_9^{\mathrm{R}}|_{\phi-only}\frac{f_+}{V_{cs}^* V_{us}}\,. \tag{26}$$

Here we neglect all resonances other than the ϕ as the latter is dominant on the ϕ, and the ρ, as it is wide. To avoid double-counting we drop the perturbative contributions to $C_9^{\mathrm{eff}(d,s)}$ in $c_{d,s}$, respectively. The resonance contributions allow to evade the otherwise strong GIM-suppression, a feature already exploited in probing BSM CP-violation in dipole operators on or near the ϕ resonance [35]. In the SM CP-violation is tiny due to the smallness of $\mathrm{Im}[V_{cd}^* V_{ud}(V_{cs} V_{us}^*)]$. We find $|A_{CP}^{\rm SM}(q^2)| < 5 \cdot 10^{-3}$, peaking at $q^2 \sim m_\phi^2$, where we normalized to the sum of the widths integrated over the full q^2-region. We conclude that while there are large uncertainties related to the phenomenological model for C_9^{R}, it allows to see large BSM effects. We show this explicitly in Sec. III, where we also study LFV decays.

III. BEYOND THE STANDARD MODEL

We discuss testable BSM effects model-independently in Sec. III A and within leptoquark models, which are introduced briefly in Sec. III B, in Sec. III C.

A. Model-independent Analysis

To study BSM effects we extend the operator basis (17)-(19)

$$\mathcal{L}_{\rm eff}^{\rm weak}(\mu\sim m_c)=\frac{4G_F}{\sqrt{2}}\frac{\alpha_e}{4\pi}\sum_i C_i^{(l)}Q_i^{(l)}\,,\qquad (c\to ul^+l^-)\,,\tag{27}$$

where

$$\begin{aligned}
Q_9^{(l)}&=(\bar u\gamma_\mu P_L c)\left(\bar l\gamma^\mu l\right)\,, & Q_9^{(l)\prime}&=(\bar u\gamma_\mu P_R c)\left(\bar l\gamma^\mu l\right)\,,\\
Q_{10}^{(l)}&=(\bar u\gamma_\mu P_L c)\left(\bar l\gamma^\mu\gamma_5 l\right)\,, & Q_{10}^{(l)\prime}&=(\bar u\gamma_\mu P_R c)\left(\bar l\gamma^\mu\gamma_5 l\right)\,,\\
Q_S^{(l)}&=(\bar u P_R c)\left(\bar l l\right)\,, & Q_S^{(l)\prime}&=(\bar u P_L c)\left(\bar l l\right)\,,\\
Q_P^{(l)}&=(\bar u P_R c)\left(\bar l\gamma_5 l\right)\,, & Q_P^{(l)\prime}&=(\bar u P_L c)\left(\bar l\gamma_5 l\right)\,,\\
Q_T^{(l)}&=\frac12(\bar u\sigma^{\mu\nu}c)\left(\bar l\sigma_{\mu\nu}l\right)\,, & Q_{T5}^{(l)}&=\frac12(\bar u\sigma^{\mu\nu}c)\left(\bar l\sigma_{\mu\nu}\gamma_5 l\right)\,.
\end{aligned}\tag{28}$$

As we use muonic modes frequently, in the following Wilson coefficients and operators without a lepton flavor index are understood as muonic ones, that is $C_i^{(\mu)}=C_i$ etc.

Neglecting the SM Wilson coefficients, we find the following constraints on the BSM Wilson coefficients from the limits on the branching fraction of $D^+\to\pi^+\mu^+\mu^-$ given in Table II in the high q^2-region ($\sqrt{q^2}\geq 1.25\,\text{GeV}$) at CL=90%

$$\begin{aligned}
&0.9|C_9+C_9'|^2+0.9|C_{10}+C_{10}'|^2+4.1|C_S+C_S'|^2+4.2|C_P+C_P'|^2+1.1|C_T|^2+1.0|C_{T5}|^2\\
&+0.6\,\text{Re}[(C_9+C_9')C_T^*]+1.2\,\text{Re}[(C_{10}+C_{10}')(C_P+C_P')^*]\\
&+2.3|C_7|^2+2.8\text{Re}[C_7(C_9+C_9')^*]+0.8\,\text{Re}[C_7C_T^*]\lesssim 1\,.
\end{aligned}\tag{29}$$

Analogous constraints in the full q^2-region are somewhat stronger. They read

$$\begin{aligned}
&1.3|C_9+C_9'|^2+1.4|C_{10}+C_{10}'|^2+2.2|C_S+C_S'|^2+2.3|C_P+C_P'|^2+0.9|C_T|^2+0.8|C_{T5}|^2\\
&+0.9\,\text{Re}[(C_9+C_9')C_T^*]+1.0\,\text{Re}[(C_{10}+C_{10}')(C_P+C_P')^*]\\
&+3.7|C_7|^2+4.4\text{Re}[C_7(C_9+C_9')^*]+1.3\,\text{Re}[C_7C_T^*]\lesssim 1\,.
\end{aligned}\tag{30}$$

The branching fraction $\mathcal{B}(D^0\to\mu^+\mu^-)<6.2\cdot10^{-9}$ at CL=90% [31] provides complementary constraints as

$$|C_S-C_S'|^2+|C_P-C_P'+0.1(C_{10}-C_{10}')|^2\lesssim 0.007\,.\tag{31}$$

Thus, $D\to\pi\mu\mu$ is sensitive to the complete set of operators, however, the purely leptonic decays put stronger constraints on scalar/pseudoscalar operators.

Barring cancellations, we find, consistent with [36], $|C_{9,10}^{(\prime)}|\lesssim 1$, which can exceed the resonance contribution at high q^2. Assuming no further flavor suppression for the BSM contribution g^2/Λ^2 (weakly-induced tree level) or $g^4/(16\pi^2\Lambda^2)$ (weak loop), the limits on $C_{9,10}^{(\prime)}$ imply quite mild constraints for the scale of new physics: $\Lambda\gtrsim\mathcal{O}(5)$ TeV or Λ around the electroweak scale, respectively. With $SU(2)_L$-relations $C_9=-C_{10}$ the bounds on new physics ease by a factor of $1/\sqrt{2}$. Analogous constraints on the other coefficients read $|C_{T,T5}|\lesssim 1$ and $|C_{S,P}^{(\prime)}|\lesssim 0.1$. In Fig. 3 we illustrate BSM effects in the $D^+\to\pi^+\mu^+\mu^-$ differential branching fraction at high q^2 with two viable choices for BSM-induced Wilson coefficients. As anticipated, the BSM distributions can exceed the SM one.

Constraints on $c\to uee$ modes are weaker than the $c\to u\mu\mu$ ones, $\mathcal{B}(D^+\to\pi^+e^+e^-)<1.1\cdot10^{-6}$ and $\mathcal{B}(D^0\to e^+e^-)<7.9\cdot10^{-8}$ at CL=90% [31], and imply

$$\begin{aligned}
&\left|C_{S,P}^{(e)}-C_{S,P}^{(e)\prime}\right|\lesssim 0.3\,,\\
&\left|C_{9,10}^{(e)}-C_{9,10}^{(e)\prime}\right|\lesssim 4\,,\quad \left|C_{T,T5}^{(e)}\right|\lesssim 5\,,\quad \left|C_7\left(C_9^{(e)}-C_9^{(e)\prime}\right)\right|\lesssim 2\,.
\end{aligned}\tag{32}$$

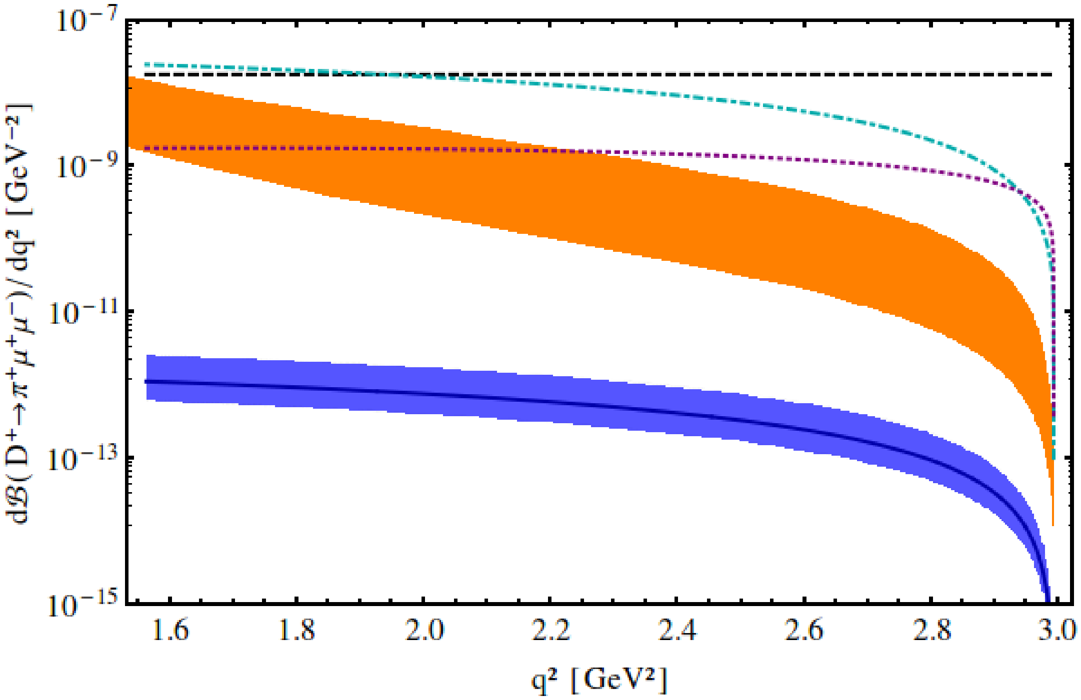

FIG. 3: The differential branching fraction $\mathrm{d}\mathcal{B}(D^+ \to \pi^+\mu^+\mu^-)/\mathrm{d}q^2$ at high q^2. The solid blue curve is the non-resonant SM prediction at $\mu_c = m_c$ and the lighter blue band its μ_c-uncertainty, the dashed black line denotes the 90% CL experimental upper limit [30] and the orange band shows the resonant contributions. The additional curves illustrate two viable, sample BSM scenarios, $|C_9| = |C_{10}| = 0.6$ (dot-dashed cyan curve) and $|C_i^{(\prime)}| = 0.04$ (dotted purple curve). In the latter case all BSM coefficients have been set simultaneously to this value.

To discuss LFV we introduce the following effective Lagrangian

$$\mathcal{L}_{\text{eff}}^{\text{weak}}(\mu \sim m_c) = \frac{4G_F}{\sqrt{2}}\frac{\alpha_e}{4\pi}\sum_i \left(K_i^{(e)}O_i^{(e)} + K_i^{(\mu)}O_i^{(\mu)}\right), \qquad (c \to u e^\pm \mu^\mp), \tag{33}$$

where the $K_i^{(l)}$ denote Wilson coefficients and the operators $O_i^{(l)}$ read

$$O_9^{(e)} = (\bar{u}\gamma_\mu P_L c)(\bar{e}\gamma^\mu \mu), \qquad O_9^{(\mu)} = (\bar{u}\gamma_\mu P_L c)(\bar{\mu}\gamma^\mu e), \tag{34}$$

and all others in analogous notation to Eq. (28). The LFV Wilson coefficients are constrained by $\mathcal{B}(D^0 \to e^+\mu^- + e^-\mu^+) < 2.6 \cdot 10^{-7}$, $\mathcal{B}(D^+ \to \pi^+e^+\mu^-) < 2.9 \cdot 10^{-6}$ and $\mathcal{B}(D^+ \to \pi^+e^-\mu^+) < 3.6 \cdot 10^{-6}$ at CL=90% [31] as

$$\begin{aligned} &\left|K_{S,P}^{(l)} - K_{S,P}^{(l)\prime}\right| \lesssim 0.4, \\ &\left|K_{9,10}^{(l)} - K_{9,10}^{(l)\prime}\right| \lesssim 6, \quad \left|K_{T,T5}^{(l)}\right| \lesssim 7, \qquad l = e, \mu. \end{aligned} \tag{35}$$

The observables in the $D \to Pl^+l^-$ angular distribution, $A_{\rm FB}$ and F_H, Eqs. (D2), (D3) can be sizable while respecting the model-independent bounds. We find that, upon q^2-integration, $|A_{\rm FB}(D^+ \to \pi^+\mu^+\mu^-)| \lesssim 0.6$, $|A_{\rm FB}(D^+ \to \pi^+e^+e^-)| \lesssim 0.8$, $F_H(D^+ \to \pi^+\mu^+\mu^-) \lesssim 1.5$ and $F_H(D^+ \to \pi^+e^+e^-) \lesssim 1.6$, where $F_H^{\rm SM}$ is below permille level, allowing to signal BSM physics. Here, the resonance contributions have been taken into account in the normalization to the decay rate, and both numerator and denominator (the decay rate) have been integrated from $q^2_{\rm min} = 1.25^2\,\text{GeV}^2$ to $q^2_{\rm max} = (m_{D^+} - m_{\pi^+})^2$. As the LFV bounds (35) are even weaker than the ones on the dielectron modes, sizable contributions to LFV angular observables are allowed as well. Knowing the size of LFV in more than one observable would allow to pin down the operator structure and provide clues about the underlying model.

B. $c \to ull$ Generating Models

Several models generating $c \to ull$ transitions were studied, for instance, Little Higgs models [19, 29], Minimal Supersymmetric Standard Models [18, 20, 37, 38], two Higgs doublet models [37], an up vector-like quark singlet [38] and models with warped extra dimensions [39, 40]. In all models except for the supersymmetric ones the $D \to \pi l^+ l^-$ branching fraction is found to be less than the resonance contributions. In the supersymmetric models the branching ratio can be close to the experimental limits. Non-vanishing asymmetries that could be $A_{\rm FB}$, A_{CP} and the CP-asymmetry of $A_{\rm FB}$ are generically induced in BSM models [18–20, 29, 39, 40].

Here we study effects of leptoquarks generating $c \to ull$ transitions in a bottom-up approach. We note that in GUTs further model building for some representations is required [41]. For renormalizable up-type scalar and vector $SU(2)_L$ singlet, doublet and triplet leptoquarks within the SM ($SU(3)_C$, $SU(2)_L$, $U(1)_Y$) gauge group [42] we find after Fierzing the effective contributions shown in Table III. Baryon number and lepton number are conserved in the interactions. Note that models S_1 and S_2 contain two couplings each. Leptoquark effects in S_1 have been discussed in [43].

$\subset \mathcal{L}_{LQ}$	$(SU(3)_C, SU(2)_L, Y)$	effective vertices
$\left(\lambda_{S_1L}\mathbf{Q}_L^T i\tau_2 \mathbf{L}_L + \lambda_{S_1R} q_R l_R\right) S_1^\dagger$	$(3, 1, -1/3)$	$-\frac{\left(\lambda^{(ql')}_{S_1R}\right)^* \lambda^{(q'l)}_{S_1R}}{2m^2_{S_1}} \left(\bar q_R \gamma_\mu q'_R\right)\left(\bar l_R \gamma^\mu l'_R\right)$
		$-\frac{\left(\lambda^{(ql')}_{S_1L}\right)^* \lambda^{(q'l)}_{S_1L}}{2m^2_{S_1}} \left(\bar q_L \gamma_\mu q'_L\right)\left(\bar l_L \gamma^\mu l'_L\right)$
		$-\frac{\left(\lambda^{(ql')}_{S_1R}\right)^* \lambda^{(q'l)}_{S_1L}}{2m^2_{S_1}} \left(\bar q_L q'_R\right)\left(\bar l_L l'_R\right)$
		$-\frac{\left(\lambda^{(ql')}_{S_1L}\right)^* \lambda^{(q'l)}_{S_1R}}{2m^2_{S_1}} \left(\bar q_R q'_L\right)\left(\bar l_R l'_L\right)$
		$-\frac{\left(\lambda^{(ql')}_{S_1R}\right)^* \lambda^{(q'l)}_{S_1L}}{8m^2_{S_1}} \left(\bar q \sigma_{\mu\nu} q'\right)\left(\bar l_L \sigma^{\mu\nu} l'_R\right)$
		$-\frac{\left(\lambda^{(ql')}_{S_1L}\right)^* \lambda^{(q'l)}_{S_1R}}{8m^2_{S_1}} \left(\bar q \sigma_{\mu\nu} q'\right)\left(\bar l_R \sigma^{\mu\nu} l'_L\right)$
$\left(\lambda_{S_2L}\bar q_R \mathbf{L}_L + \lambda_{S_2R}\bar{\mathbf{Q}}_L i\tau_2 l_R\right) S_2^\dagger$	$(3, 2, -7/6)$	$-\frac{\lambda^{(ql')}_{S_2R}\left(\lambda^{(q'l)}_{S_2R}\right)^*}{2m^2_{S_2}} \left(\bar q_L \gamma_\mu q'_L\right)\left(\bar l_R \gamma^\mu l'_R\right)$
		$-\frac{\lambda^{(ql')}_{S_2L}\left(\lambda^{(q'l)}_{S_2L}\right)^*}{2m^2_{S_2}} \left(\bar q_R \gamma_\mu q'_R\right)\left(\bar l_L \gamma^\mu l'_L\right)$
		$-\frac{\lambda^{(ql')}_{S_2R}\left(\lambda^{(q'l)}_{S_2L}\right)^*}{2m^2_{S_2}} \left(\bar q_L q'_R\right)\left(\bar l_L l'_R\right)$
		$-\frac{\lambda^{(ql')}_{S_2L}\left(\lambda^{(q'l)}_{S_2R}\right)^*}{2m^2_{S_2}} \left(\bar q_R q'_L\right)\left(\bar l_R l'_L\right)$
		$-\frac{\lambda^{(ql')}_{S_2R}\left(\lambda^{(q'l)}_{S_2L}\right)^*}{8m^2_{S_2}} \left(\bar q \sigma_{\mu\nu} q'\right)\left(\bar l_L \sigma^{\mu\nu} l'_R\right)$
		$-\frac{\lambda^{(ql')}_{S_2L}\left(\lambda^{(q'l)}_{S_2R}\right)^*}{8m^2_{S_2}} \left(\bar q \sigma_{\mu\nu} q'\right)\left(\bar l_R \sigma^{\mu\nu} l'_L\right)$
$\left(\lambda_{S_3}\mathbf{Q}_L^T i\tau_2 \vec\tau \mathbf{L}_L\right) \cdot \vec{S_3}^\dagger$	$(3, 3, -1/3)$	$-\frac{\left(\lambda^{(ql')}_{S_3}\right)^* \lambda^{(q'l)}_{S_3}}{2m^2_{S_3}} \left(\bar q_L \gamma_\mu q'_L\right)\left(\bar l_L \gamma^\mu l'_L\right)$
$\lambda_{\tilde V_1}\bar q_R \gamma_\mu l_R \left(\tilde V_1^\mu\right)^\dagger$	$(3, 1, -5/3)$	$\frac{\lambda^{(ql')}_{\tilde V_1}\left(\lambda^{(q'l)}_{\tilde V_1}\right)^*}{m^2_{\tilde V_1}} \left(\bar q_R \gamma_\mu q'_R\right)\left(\bar l_R \gamma^\mu l'_R\right)$
$\lambda_{V_2}\mathbf{Q}_L \gamma_\mu l_R \left(V_2^\mu\right)^\dagger$	$(3, 2, -5/6)$	$\frac{\left(\lambda^{(ql')}_{V_2}\right)^* \lambda^{(q'l)}_{V_2}}{m^2_{V_2}} \left(\bar q_L \gamma_\mu q'_L\right)\left(\bar l_R \gamma^\mu l'_R\right)$
$\lambda_{\tilde V_2} q_R \gamma_\mu \mathbf{L}_L \left(\tilde V_2^\mu\right)^\dagger$	$(3, 2, 1/6)$	$\frac{\left(\lambda^{(ql')}_{\tilde V_2}\right)^* \lambda^{(q'l)}_{\tilde V_2}}{m^2_{\tilde V_2}} \left(\bar q_R \gamma_\mu q'_R\right)\left(\bar l_L \gamma^\mu l'_L\right)$
$\lambda_{V_3}\bar{\mathbf{Q}}_L \gamma_\mu \vec\tau \mathbf{L}_L \cdot \left(\vec{V_3}^\mu\right)^\dagger$	$(3, 3, -2/3)$	$\frac{2\lambda^{(ql')}_{V_3}\left(\lambda^{(q'l)}_{V_3}\right)^*}{m^2_{V_3}} \left(\bar q_L \gamma_\mu q'_L\right)\left(\bar l_L \gamma^\mu l'_L\right)$

TABLE III: Leptoquark-fermion interactions, quantum numbers, with hypercharge $Y = Q_e - T_3$, and effective $c \to u (l')^+ l^-$ vertices via Fierz identities. $\tau_a, a = 1, 2, 3$ denote the Pauli matrices, and $\vec\tau \cdot \vec X = \sum_a \tau_a X_a$ for $X = S_3, V_3$. SM $SU(2)_L$-doublets are $\mathbf{Q}(3, 2, 1/6)$ and $\mathbf{L}(1, 2, -1/2)$, $q, q' = u, c$, and $l, l' = e, \mu$.

We uniformly denote by M the mass of the leptoquarks but note that they differ in general depending on the representation. We assume degenerate $SU(2)_L$-plet masses to comply with the constraints from oblique parameters [44]. Our effective vertices agree with and extend those in [45] by considering tensor operators and relative signs. The Wilson coefficients induced by tree-level leptoquark exchanges read as

$$
\begin{aligned}
C_{9,10} &= \frac{\sqrt{2}\pi}{G_F\alpha_e} k_{9,10} \frac{\lambda_i^I \left(\lambda_i^J\right)^*}{M^2}\,, & C'_{9,10} &= \frac{\sqrt{2}\pi}{G_F\alpha_e} k'_{9,10} \frac{\lambda_j^I \left(\lambda_j^J\right)^*}{M^2}\,, \\
C_S = C_P &= \frac{\sqrt{2}\pi}{G_F\alpha_e} k_{S,P} \frac{\lambda_i^I \left(\lambda_j^J\right)^*}{M^2}\,, & C'_S = -C'_P &= \frac{\sqrt{2}\pi}{G_F\alpha_e} k'_{S,P} \frac{\lambda_j^I \left(\lambda_i^J\right)^*}{M^2}\,, \\
C_T &= \frac{\sqrt{2}\pi}{G_F\alpha_e} k_T \left(\frac{\lambda_i^I \left(\lambda_j^J\right)^*}{M^2} + \frac{\lambda_j^I \left(\lambda_i^J\right)^*}{M^2}\right), & C_{T5} &= \frac{\sqrt{2}\pi}{G_F\alpha_e} k_{T5} \left(\frac{\lambda_i^I \left(\lambda_j^J\right)^*}{M^2} - \frac{\lambda_j^I \left(\lambda_i^J\right)^*}{M^2}\right),
\end{aligned}
\tag{36}
$$

where $i,j = L,R$; such indices are nontrivial for scenarios S_1 and S_2 only, which have two different couplings $\lambda_{L,R}$ each. The correct values of i,j can also be read off from Table III. The coefficients k_x are given in Table IV.

	I	J	i	j	k_9	k_{10}	k'_9	k'_{10}	$k_{S,P}$	$k'_{S,P}$	k_T	k_{T5}
S_1	(cl)	(ul)	L	R	$-\frac{1}{4}$	$\frac{1}{4}$	$-\frac{1}{4}$	$-\frac{1}{4}$	$-\frac{1}{4}$	$-\frac{1}{4}$	$-\frac{1}{8}$	$-\frac{1}{8}$
S_2	(ul)	(cl)	R	L	$-\frac{1}{4}$	$-\frac{1}{4}$	$-\frac{1}{4}$	$\frac{1}{4}$	$-\frac{1}{4}$	$-\frac{1}{4}$	$-\frac{1}{8}$	$-\frac{1}{8}$
S_3	(cl)	(ul)	L	–	$-\frac{1}{4}$	$\frac{1}{4}$	0	0	0	0	0	0
$\tilde{V}_1$	(ul)	(cl)	–	R	0	0	$\frac{1}{2}$	$\frac{1}{2}$	0	0	0	0
V_2	(cl)	(ul)	R	–	$\frac{1}{2}$	$\frac{1}{2}$	0	0	0	0	0	0
$\tilde{V}_2$	(cl)	(ul)	–	L	0	0	$\frac{1}{2}$	$-\frac{1}{2}$	0	0	0	0
V_3	(ul)	(cl)	L	–	1	-1	0	0	0	0	0	0

TABLE IV: Coefficient matrix for the leptoquark Wilson coefficients (36) inducing $c \to ull$.

C. Leptoquark Phenomenology

Experimental constraints on leptoquark couplings are worked out in App. F. While generically $|\lambda^{(ql)}| \lesssim \mathcal{O}(0.1)\,[M/\mathrm{TeV}]$ for any coupling to the first two generations and for any scenario of Table III, several flavor-combinations are more severely constrained. In addition, bounds for specific models making use of correlations can be much stronger.

The $|\Delta C| = |\Delta U| = 1$ couplings in leptoquark scenarios involving doublet-quarks $\mathbf{Q}$ are subject to constraints from the kaon sector (Table XV). Corresponding limits on the Wilson coefficients for $c \to ull^{(\prime)}$ are given in Table V. Only the scenarios $\tilde{V}_1$ and $\tilde{V}_2$, as well as the $S_1|_R$ and $S_2|_L$ couplings do not receive such constraints, hence allow in general for larger effects for $c \to ull$, however, decouple without further input from the K- and B-sector.

	(ee)	$(e\mu), (\mu e)$	$(\mu\mu)$
$S_1\|_L$	$\lesssim 4 \cdot 10^{-3}$	$\lesssim 4 \cdot 10^{-3}$	$\lesssim 4 \cdot 10^{-3}$
$S_2\|_R$, V_2	$\lesssim 3 \cdot 10^{-2}$	$\lesssim 2 \cdot 10^{-4}$	$\lesssim 4 \cdot 10^{-3}$
S_3, V_3	$\lesssim 4 \cdot 10^{-3}$	$\lesssim 2 \cdot 10^{-4}$	$\lesssim 4 \cdot 10^{-3}$

TABLE V: Upper limits on the $c \to ull^{(\prime)}$ Wilson coefficients $|C_{9,10}^{(\prime)}|$ abbreviated as $(ll^{(\prime)})$ in leptoquark scenarios from kaon decays. For $S_{1,2}$ the limits apply to the indicated handedness of couplings only.

Products of two Wilson coefficients are constrained by the strong limits on $\mu - e$ conversion and $\mu \to e\gamma$, see Table VI. Future experiments on $\mu \to e\gamma$ [46] and $\mu - e$ conversion [47, 48] can improve the limits by at least two orders of magnitude.

Further bounds and correlations depend on the flavor structure. To make progress here we study benchmark patterns of leptoquark coupling matrices λ put forward in [49] for quark-$\mathbf{L}$-type Yukawa couplings based on flavor symmetries. Rows label quark flavors and columns label lepton flavors. The use of discrete non-abelian symmetries for the leptons, specifically A_4 [50, 51], results in textures with "ones" and "zeros", very different from hierarchical ones in Froggatt-Nielsen $U(1)$-models [52]. In this work we are mainly concerned with the first two generations, so

	$(ee)(\mu\mu)$, $(e\mu)(\mu e)$
S_1	$\lesssim 2\cdot 10^{-7}$
S_2	$\lesssim 8\cdot 10^{-8}$
S_3, $\tilde V_1$, V_2, $\tilde V_2$, V_3	$\lesssim 6\cdot 10^{-8}$
$S_1\|_{LR}$, $S_2\|_{LR}$	$\lesssim 2\cdot 10^{-10}$

TABLE VI: Upper limits on the products of two $c\to ull^{(\prime)}$ Wilson coefficients $|C_i^{(e)(\prime)}C_i^{(\mu)(\prime)}|$, "$(ee)(\mu\mu)$", and $|K_i^{(e)(\prime)}K_i^{(\mu)(\prime)}|$, "$(e\mu)(\mu e)$", from $\mu-e$ conversion and $\mu\to e\gamma$. The LR-mixing constraints in scenarios $S_{1,2}$ are stronger than the unmixed ones and are given in the last row.

our terminology reflects features of the upper left two-by-two submatrix of λ. With the exception of $D^0\to\tau e$ and $c\to u\nu\bar\nu$, the third (τ,ν_τ) column is irrelevant to our study. Similar statements hold for the third (t,b) row, which is relevant to B-physics, and is linked to charm physics via flavor. We define

i) a hierarchical flavor pattern with suppression factors for electrons, κ, and first and second generation quarks, ρ_d and ρ, respectively,

$$\lambda_i \sim \begin{pmatrix} \rho_d\kappa & \rho_d & \rho_d \\ \rho\kappa & \rho & \rho \\ \kappa & 1 & 1 \end{pmatrix}, \tag{37}$$

ii) a single lepton pattern with negligible electron couplings

$$\lambda_{ii} \sim \begin{pmatrix} 0 & * & 0 \\ 0 & * & 0 \\ 0 & * & 0 \end{pmatrix}, \tag{38}$$

and iii) a (first two) generation-diagonal "skewed" pattern, that is, $\lambda^{(u\mu)}$ and $\lambda^{(ce)}$ are negligible

$$\lambda_{iii} \sim \begin{pmatrix} * & 0 & 0 \\ 0 & * & 0 \\ 0 & * & 0 \end{pmatrix}. \tag{39}$$

The patterns i) and ii) have been explicitly obtained in models where quarks are A_4-singlets, hence apply to all u_R, d_R and $\mathbf{Q}$ fields coupling to lepton doublets.[2] Extension of [49] to include lepton singlets as well as the skewed patterns iii) and iv), the latter defined in Eq. (41), is not as strainghforward and requires further model building, which is beyond the scope of this work. (Note that skewed patterns have been obtained by assigning different quark generations to different A_4 singlet representations [49].)

Upper limits on rare charm branching fractions for different flavor patterns are given in Table VII. Here, for patterns ii) and iii) we distinguish between leptoquark scenarios which can escape kaon bounds, $S_{1,2}$, $\tilde V_{1,2}$, ii.1) and iii.1), and those subject to kaon bounds, S_3, $V_{2,3}$, ii.2) and iii.2). If κ is small the hierarchical flavor pattern i) effectively reduces to pattern ii).

The $c\to ue^+e^-$ Wilson coefficients vanish in patterns ii) and iii). In pattern i) they are driven by $\rho_d\rho\kappa^2$, and correlated with LFV, hence subject to the bounds in Table VI. We find that no BSM signal can be seen in $c\to ue^+e^-$ branching ratios.

In pattern ii.1) the muon Wilson coefficients are constrained by $D^+\to\pi^+\mu^+\mu^-$ and $D^0\to\mu^+\mu^-$ as discussed in Sec. III A. For ii.2) the constraints on the muon Wilson coefficients are given in Table V. In case of iii) the $c\to u\mu^+\mu^-$ Wilson coefficients vanish.

The dineutrino mode is induced in $S_{2,3}$, $\tilde V_2$ and V_3 models because those contain the requisite electromagnetic charge $+2/3e$ leptoquark. The decay $D\to\pi\nu\bar\nu$ has backgrounds from $D\to\tau(\to\pi\nu)\bar\nu$, which can be controlled by kinematic cuts $q^2>(m_\tau^2-m_{\pi^+}^2)(m_{D^+}^2-m_\tau^2)/m_\tau^2\simeq 0.34\,\mathrm{GeV}^2$ [18, 53].

The LFV transition $c\to u\mu^-e^+$ ($c\to u\mu^+e^-$) is mediated by a generation-diagonally coupling leptoquark with electric charge $5/3e$ ($-1/3e$). Therefore, for case iii) either, for charge $-1/3e$, $\mathcal{B}(D^0\to\mu^-e^+)$ and $\mathcal{B}(\bar D^0\to\mu^+e^-)$

[2] We thank Ivo de Medeiros Varzielas for confirmation.

vanish, or, for charge $5/3e$, $\mathcal{B}(D^0 \to \mu^+ e^-)$ and $\mathcal{B}(\bar{D}^0 \to \mu^- e^+)$ vanish. Analogous statements hold for $D^+ \to \pi^+ e^\pm \mu^\mp$ decays. For iii.1) the LFV Wilson coefficients are $\lesssim \mathcal{O}(1-10)$, see Eq. (35), and for iii.2) the constraints on the LFV Wilson coefficients from Table V apply. For ii) the LFV Wilson coefficients vanish.

	$\mathcal{B}(D^+ \to \pi^+\mu^+\mu^-)$	$\mathcal{B}(D^0 \to \mu^+\mu^-)$	$\mathcal{B}(D^+ \to \pi^+ e^\pm \mu^\mp)$	$\mathcal{B}(D^0 \to \mu^\pm e^\mp)$	$\mathcal{B}(D^+ \to \pi^+ \nu\bar{\nu})$
i)	SM-like	SM-like	$\lesssim 2 \cdot 10^{-13}$	$\lesssim 7 \cdot 10^{-15}$	$\lesssim 3 \cdot 10^{-13}$
ii.1)	$\lesssim 7 \cdot 10^{-8}$ $(2 \cdot 10^{-8})$	$\lesssim 3 \cdot 10^{-9}$	0	0	$\lesssim 8 \cdot 10^{-8}$
ii.2)	SM-like	$\lesssim 4 \cdot 10^{-13}$	0	0	$\lesssim 4 \cdot 10^{-12}$
iii.1)	SM-like	SM-like	$\lesssim 2 \cdot 10^{-6}$	$\lesssim 4 \cdot 10^{-8}$	$\lesssim 2 \cdot 10^{-6}$
iii.2)	SM-like	SM-like	$\lesssim 8 \cdot 10^{-15}$	$\lesssim 2 \cdot 10^{-16}$	$\lesssim 9 \cdot 10^{-15}$

TABLE VII: Branching fractions for the full q^2-region (high q^2-region) for different classes of leptoquark couplings, see text. Summation of neutrino flavors is understood. "SM-like" denotes a branching ratio which is dominated by resonances or is of similar size as the resonance-induced one. All $c \to u e^+ e^-$ branching ratios are "SM-like" in the models considered. Note that in the SM $\mathcal{B}(D^0 \to \mu\mu) \sim 10^{-13}$ [18].

Complex couplings are additionally constrained by electron and neutron electric dipole moments as $\mathrm{Im}[C_i^{(e)}] \lesssim 4 \cdot 10^{-9}$ and $\mathrm{Im}[C_i^{(\mu)}] \lesssim 4 \cdot 10^{-6}$, $i = S, P, T, T5$, respectively. The $D^+ \to \pi^+\mu^+\mu^-$ CP-asymmetry in the rate, Eq. (23), is shown for the muons-only pattern ii) in Fig. 4. Around the ϕ-resonance (left-handed plots), A_{CP} scales with the BSM coefficient Δ_9, as the normalization is driven by the resonances, C_9^R, for any BSM coefficient. At high q^2 (right-handed plots) the normalization depends on the value of Δ_9. In the plot to the upper right the normalization is set by Δ_9, hence A_{CP} becomes inversely proportional to Δ_9. In the plot to the lower right, corresponding to a scenario with smaller BSM effects, ii.2), the normalization is again dominated by the resonances. Despite the constrained Wilson coefficients the CP-asymmetry can be sizable around the ϕ and above in the high q^2-region, in which $|A_{CP}|$ drops towards the endpoint. If measured around the ϕ, a sizable CP-asymmetry, while assuming different values, can arise independent of the strong phases. For the hierarchical pattern i) $|A_{CP}|$ is $\lesssim 0.003$ on the ϕ-resonance and $\lesssim 0.03$ at high q^2.

Interestingly, there exists an opportunity to also study τ-lepton couplings in charm, with $D^0 \to \tau^\pm e^\mp$ decays. The corresponding branching fractions can be inferred from Eq. (D6); the phase space suppression relative to $D^0 \to \mu^\pm e^\mp$ is about $8 \cdot 10^{-3}$. We find, approximately,

$$\mathcal{B}(D^0 \to \tau^\pm e^\mp) \simeq 5 \cdot 10^{-9} \left(\left| 1.3 \left(K_S^{(e,\tau)} - K_S^{(e,\tau)\prime} \right) \mp \left(K_9^{(e,\tau)} - K_9^{(e,\tau)\prime} \right) \right|^2 + \left| 1.3 \left(K_P^{(e,\tau)} - K_P^{(e,\tau)\prime} \right) + \left(K_{10}^{(e,\tau)} - K_{10}^{(e,\tau)\prime} \right) \right|^2 \right) . \tag{40}$$

The limits on the decays $\tau \to e\gamma$ and $\tau \to eee$ are not competitive with those involving muons, however, $SU(2)$-relations imply constraints on LFV. For (axial)vector couplings they read $|K_{9,10}^{(e,\tau)(\prime)}| \lesssim 0.2$ $(\mathcal{B}(\tau \to eK))$, significantly weaker than $|K_{9,10}^{(e,\tau)}| \lesssim 4 \cdot 10^{-3}$ $(\mathcal{B}(K^+ \to \pi^+\bar{\nu}\nu))$ and for (pseudo)scalar Wilson coefficients $|K_{S,P}^{(e,\tau)(\prime)}| \lesssim 7 \cdot 10^{-3}$ $(\mathcal{B}(K^+ \to \bar{e}\nu))$ [54]. The hierarchical flavor pattern yields $\mathcal{B}(D^0 \to \tau^\pm e^\mp) \lesssim 7 \cdot 10^{-15}$, while the others, ii) and iii), give vanishing rates. One flavor pattern in which the $SU(2)$-related constraints are absent and which can signal LFV BSM $D^0 \to \tau^\pm e^\mp$ decays, is another skewed one, inspired by [49],

$$\lambda_{iv} \sim \begin{pmatrix} 0 & 0 & * \\ * & 0 & 0 \\ * & 0 & 0 \end{pmatrix} . \tag{41}$$

This pattern results in SM-like lepton-diagonal $c \to u l^+ l^-$, $l = e, \mu$ and vanishing flavor off-diagonal $c \to u e^\pm \mu^\mp$ modes, while $\mathcal{B}(D \to \pi\nu\bar{\nu})$ can exceed the upper limits given in Table VII. Other flavor patterns result in a different phenomenology, hence, if measured, this allows to learn about flavor.

IV. SUMMARY

Rare charm decays into leptons offer genuine avenues to search for BSM physics despite notorious resonance backgrounds. Semileptonic branching ratios $D \to \pi l^+ l^-$ can signal BSM physics above the ϕ-resonance right around

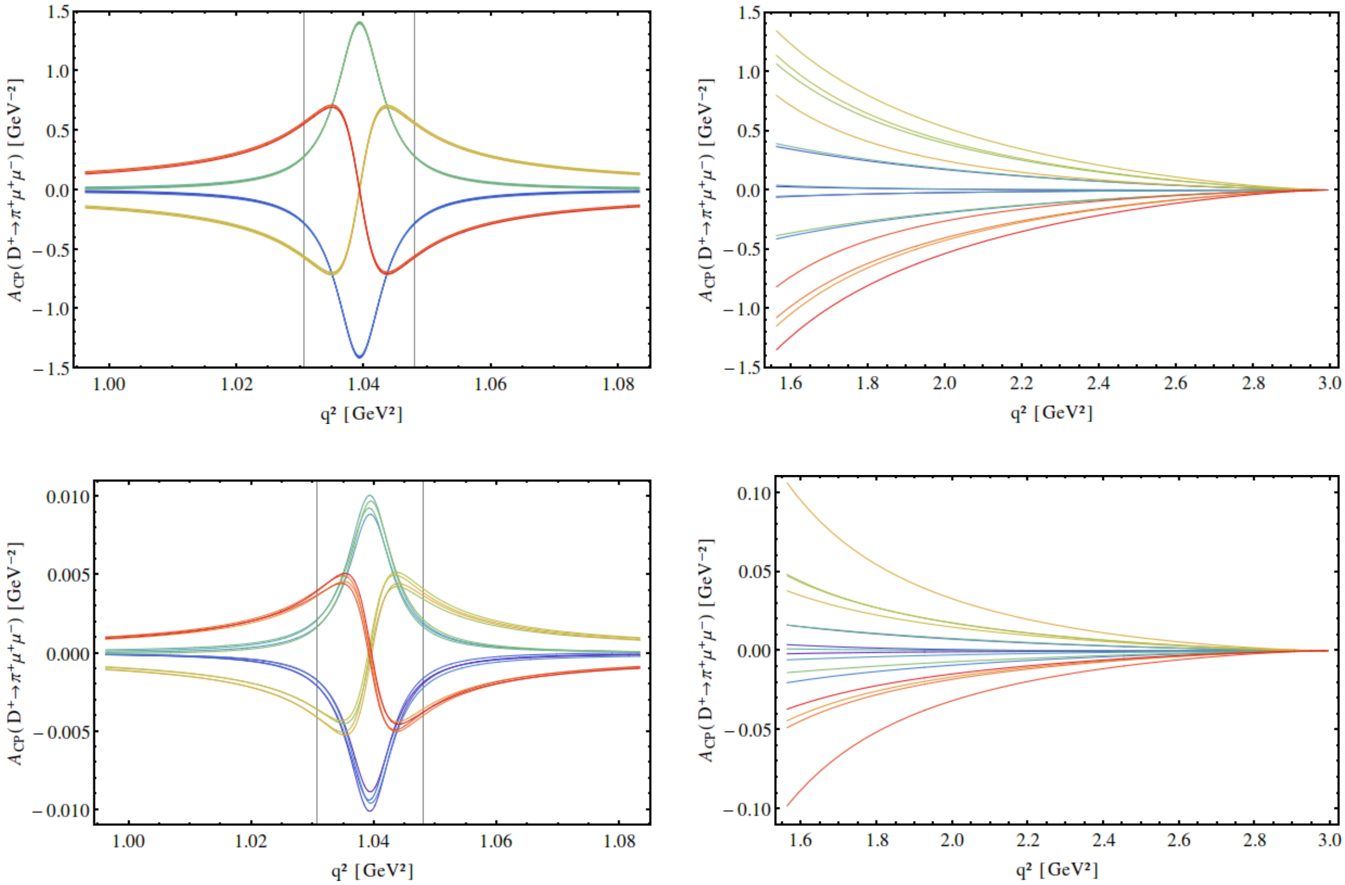

FIG. 4: The direct CP-asymmetry $A_{CP}(D^+ \to \pi^+\mu^+\mu^-)$ normalized to $[q^2_{\rm min} = (m_\phi - 5\Gamma_\phi)^2,\, q^2_{\rm max} = (m_\phi + 5\Gamma_\phi)^2]$ (left plots) and $[q^2_{\rm min} = 1.25^2\,\mathrm{GeV}^2,\, q^2_{\rm max} = (m_{D^+} - m_{\pi^+})^2]$ (right plots) in case of ii.1) (upper plots) and ii.2) (lower plots) for independent relative strong phases $\delta_{\rho,\phi} \in \{0, \pi/2, \pi, 3\pi/2\}$. From yellow (upper curves above ϕ) to red (lower curves above ϕ) each bunch represents $\delta_\phi = \pi/2, \pi, 0, 3/2\pi$.

the current experimental limit for large BSM contributions, see Fig. 3. CP-asymmetries, assisted by the resonances, observables in the angular distribution, dineutrino modes and LFV ones can signal BSM physics for much smaller BSM contributions, because those correspond to SM null tests. Model-independent constraints are given in Sec. III A.

We work out correlations in several flavor benchmarks for scalar and vector leptoquark scenarios that induce $c \to ull^{(\prime)}$ modes. The main results on the leptoquark phenomenology are given in Sec. III C. We find that hierarchical flavor patterns such as (37) allow only for rather limited effects in charm due to the correlations with other sectors which are subject to strong constraints. Other flavor patterns can give larger effects in branching ratios for decays into dimuons, dineutrinos and LFV ones, see Table VII. The CP-asymmetry in the $D^+ \to \pi^+\mu^+\mu^-$ rate provides an opportunity to probe new physics even for rather suppressed couplings in case of leptoquarks coupling to $SU(2)$-doublet quarks, see the lower two plots in Fig. 4. Such asymmetries may show up, for instance, with leptoquarks $S_3(3, 3, -1/3)$ with electron couplings sufficiently suppressed, a model that can also accommodate recent LNU hints in rare $B \to Kl^+l^-$ decays [7, 8].

The benchmark patterns studied in this work do not exhaust the flavor model space. We emphasize the importance of searches for FCNCs into dineutrinos and LFV, including $D^0 \to \tau^\pm e^\mp$ decays. Further experimental and theoretical study is needed to progress with the quest for BSM and flavor physics.

Note added: Soon after we published this paper on the arXiv a related analysis [56] appeared.
Note also that the recent LHCb bound $\mathcal{B}(D^0 \to e^\pm\mu^\mp) < 1.3 \cdot 10^{-8}$ at 90 % CL [57] that appeared while this paper has been under review starts to constrain certain leptoquark flavor scenarios, see Table VII. Furthermore, the measurement of $\mathcal{B}(D^+ \to \omega\pi^+)$ reported in a recent preprint by BES III [58] yields $a_\omega = 0.032^{+0.006}_{-0.007}\,\mathrm{GeV}^2$, somewhat lower than isospin prediction reported around Eq. (22).

Acknowledgments

We thank Christoph Bobeth, Zoltan Ligeti, Bastian Müller and Dirk Seidel for useful comments on the manuscript. GH is grateful to the Kavli Institute for Theoretical Physics at Santa Barbara where parts of this project have been done for kind hospitality. This project is supported in part by the DFG Research Unit FOR 1873 "Quark Flavour Physics and Effective Field Theories" and the National Science Foundation under Grant No. NSF PHY11-25915.

Appendix A: Parameters

$\overline{MS}$ masses are taken from [31]

$$m_t(m_t) = 160^{+5}_{-4}\ \text{GeV}\,, \qquad m_b(m_b) = 4.18 \pm 0.03\ \text{GeV}\,, \tag{A1}$$

$$m_c(m_c) = 1.275 \pm 0.025\ \text{GeV}\,, \qquad m_s(2\ \text{GeV}) = 0.095 \pm 0.005\ \text{GeV}\,. \tag{A2}$$

The NNLO running, decoupling at flavor thresholds and quark pole mass is taken from [55]. The CKM matrix is given by the UTfit collaboration [59]. The inclusive semileptonic branching fractions are given by the PDG [31], where we use $\mathcal{B}(D \to X l^+ \nu_l) = \mathcal{B}(D \to X l^+)$, consistent with [60], and employ $\mathcal{B}(D_s^+ \to X \mu^+ \nu_\mu) \simeq \mathcal{B}(D_s^+ \to X e^+ \nu_e)$. The particle masses, widths and branching fractions are given by the PDG [31]. The decay constants are given by the FLAG [61] $f_D = 0.2092 \pm 0.0033\,\text{GeV}$, $f_{D_s^+} = 0.2486 \pm 0.0027\,\text{GeV}$. The bag parameter is [62] $B_{D^0}(\mu = 3\,\text{GeV}) = 0.757 \pm 0.028$. We update the nuclear weak charge of cesium [63, 64] using [31] $\Delta Q_w(\text{Cs}) = 0.69 \pm 0.44$, where $\Delta Q_w = Q_w^{\text{exp}} - Q_w^{\text{SM}}$.

The leptonic pion decay ratio $R^{\text{exp}}_{e/\mu} = \Gamma(\pi^+ \to (e^+\nu_e + e^+\nu_e\gamma))/\Gamma(\pi^+ \to (\mu^+\nu_\mu + \mu^+\nu_\mu\gamma)) = (1.230 \pm 0.004)\cdot 10^{-4}$ [31], $R^{\text{SM}}_{e/\mu} = (1.2352 \pm 0.0001)\cdot 10^{-4}$ [65] and, thus we find $\Delta R_{e/\mu} = (-5.0 \pm 4.0)\cdot 10^{-7}$. The anomalous magnetic moment of the electron is [66] $\Delta a(e) = (-0.91 \pm 0.82)\cdot 10^{-12}$. Moreover [31]

$$\Delta a(\mu) = (288 \pm 63 \pm 49)\cdot 10^{-11}\,, \tag{A3}$$

$$|m_{D_1^0} - m_{D_2^0}| = (0.95^{+0.41}_{-0.44})\cdot 10^{10}\ \text{s}^{-1}\,, \tag{A4}$$

$$\mathcal{B}(D^+ \to \mu^+\nu_\mu) = (3.82 \pm 0.33)\cdot 10^{-4}\,, \tag{A5}$$

$$\mathcal{B}(D_s^+ \to \mu^+\nu_\mu) = (5.56 \pm 0.25)\cdot 10^{-3} \tag{A6}$$

and at CL=90% [31]

$$d(n) < 0.29 \cdot 10^{-25}\, e\ \text{cm}\,, \tag{A7}$$

$$d(e) < 10.5 \cdot 10^{-28}\, e\ \text{cm}\,, \tag{A8}$$

$$\mathcal{B}(\pi^+ \to \mu^+\nu_e) < 8.0 \cdot 10^{-3}\,, \tag{A9}$$

$$\mathcal{B}(\mu^- \to e^-\gamma) < 5.7 \cdot 10^{-13}\,, \tag{A10}$$

$$\mathcal{B}(\mu^- \to e^-e^+e^-) < 1.0 \cdot 10^{-12}\,, \tag{A11}$$

$$\Gamma(\mu^-\text{Ti} \to e^-\text{Ti})/\Gamma_{\text{capture}}(\mu^-\text{Ti}) < 4.3 \cdot 10^{-12}\,, \tag{A12}$$

$$\Gamma(\mu^-\text{Au} \to e^-\text{Au})/\Gamma_{\text{capture}}(\mu^-\text{Au}) < 7 \cdot 10^{-13}\,, \tag{A13}$$

where $\Gamma_{\text{capture}}(\mu^-\text{Ti}) = 2.59 \cdot 10^6\, s^{-1}$ and $\Gamma_{\text{capture}}(\mu^-\text{Au}) = 13.07 \cdot 10^6\, s^{-1}$ [67].

Appendix B: Effective Wilson Coefficients

In this appendix we give auxiliary functions and coefficients of the effective Wilson coefficients defined in Sec. II A. We find

$$L(m^2, q^2) = \frac{5}{3} + \ln\frac{\mu_c^2}{m^2} + x - \frac{1}{2}(2+x)|1-x|^{1/2} \begin{cases} \ln\frac{1+\sqrt{1-x}}{1-\sqrt{1-x}} - i\pi & x \equiv \frac{(2m)^2}{q^2} < 1 \\ 2\tan^{-1}\left[\frac{1}{\sqrt{x-1}}\right] & x \equiv \frac{(2m)^2}{q^2} > 1 \end{cases} \tag{B1}$$

and in the limit $m^2 = 0$

$$L(0, q^2) = \frac{5}{3} + \ln\frac{\mu_c^2}{q^2} + i\pi\,. \tag{B2}$$

We take from [12]

$$f(\rho) = -\frac{1}{243}\big((3672 - 288\pi^2 - 1296\zeta_3 + (1944 - 324\pi^2)\ln\rho + 108\ln^2\rho + 36\ln^3\rho)\rho$$
$$+ 576\pi^2\rho^{\frac{3}{2}} + (324 - 576\pi^2 + (1728 - 216\pi^2)\ln\rho + 324\ln^2\rho + 36\ln^3\rho)\rho^2$$
$$+ (1296 - 12\pi^2 + 1776\ln\rho - 2052\ln^2\rho)\rho^3\big)$$
$$- \frac{4\pi i}{81}\big((144 - 6\pi^2 + 18\ln\rho + 18\ln^2\rho)\rho + (-54 - 6\pi^2 + 108\ln\rho + 18\ln^2\rho)\rho^2$$
$$+ (116 - 96\ln\rho)\rho^3\big)$$
$$- \frac{92}{81}\ln\frac{\mu_c^2}{m_c^2} + \frac{983}{243} + \frac{52}{81}\pi i + \mathcal{O}\left((\rho\ln\rho)^4\right)\,, \tag{B3}$$

where we find the constant terms from [68]. From [16] we obtain

$$y^{(7)} = \left\{0, 0, \frac{2}{3}, \frac{8}{9}, \frac{40}{3}, \frac{160}{9}\right\}\,, \qquad y^{(8)} = \left\{0, 0, 1, -\frac{1}{6}, 20, -\frac{10}{3}\right\} \tag{B4}$$

and [25]

$$F_8^{(7)}(\rho) = \frac{8\pi^2}{27}\frac{(2+\rho)}{(1-\rho)^4} - \frac{8}{9}\frac{\left(11 - 16\rho + 8\rho^2\right)}{(1-\rho)^2} - \frac{16}{9}\frac{\sqrt{\rho}\sqrt{4-\rho}}{(1-\rho)^3}\left(9 - 5\rho + 2\rho^2\right)\arcsin\frac{\sqrt{\rho}}{2}$$
$$- \frac{32}{3}\frac{(2+\rho)}{(1-\rho)^4}\arcsin^2\frac{\sqrt{\rho}}{2} - \frac{16}{9}\frac{\rho}{(1-\rho)}\ln\rho - \frac{32}{9}\ln\frac{\mu_c^2}{m_c^2} - \frac{16}{9}\pi i\,, \tag{B5}$$

$$F_8^{(9)}(\rho) = -\frac{16\pi^2}{27}\frac{(4-\rho)}{(1-\rho)^4} + \frac{16}{9}\frac{(5-2\rho)}{(1-\rho)^2} + \frac{32}{9}\frac{\sqrt{4-\rho}}{\sqrt{\rho}(1-\rho)^3}\left(4 + 3\rho - \rho^2\right)\arcsin\frac{\sqrt{\rho}}{2}$$
$$+ \frac{64}{3}\frac{(4-\rho)}{(1-\rho)^4}\arcsin^2\frac{\sqrt{\rho}}{2} + \frac{32}{9}\frac{1}{(1-\rho)}\ln\rho\,. \tag{B6}$$

Appendix C: Form Factors

We parametrize the hadronic matrix elements in terms of the form factors $f_i(q^2)$, $i = +, T, 0$,

$$\langle P(p_P)|\bar{u}\gamma^\mu(1\pm\gamma_5)c|D(p_D)\rangle = f_+(q^2)\left(p^\mu - \frac{m_D^2 - m_P^2}{q^2}q^\mu\right) + f_0(q^2)\frac{m_D^2 - m_P^2}{q^2}q^\mu\,, \tag{C1}$$

$$\langle P(p_P)|\bar{u}\sigma^{\mu\nu}(1\pm\gamma_5)c|D(p_D)\rangle = i\frac{f_T(q^2)}{m_D}(p^\mu q^\nu - q^\mu p^\nu \pm i\epsilon^{\mu\nu\rho\sigma}p_\rho q_\sigma)\,, \tag{C2}$$

where $q^\mu = (p_D - p_P)^\mu = (p_{l^+} + p_{l^-})^\mu$ and $p^\mu = (p_D + p_P)^\mu$. For $D^0 \to \pi^0$ the form factors are scaled $f_i \to f_i/\sqrt{2}$ by isospin. The heavy-to-light form factors are related within the Heavy Quark Effective Theory by means of a heavy quark spin symmetry [69, 70]. At low recoil [71]

$$f_T(q^2) = \frac{m_D^2}{q^2}\left(1 - \frac{\alpha_s}{\pi}\frac{1}{3}\ln\frac{\mu_c^2}{m_c^2}\right)f_+(q^2) + \mathcal{O}\left(\frac{\Lambda_{\rm QCD}}{m_c}, \alpha_s^2\right)\,. \tag{C3}$$

The breaking of the heavy quark spin symmetry at large recoil reads [72]

$$f_T(q^2) = \left(1 + \frac{\alpha_s}{\pi}\left(-\frac{2}{3}\frac{2E}{m_D - 2E}\ln\frac{2E}{m_D} - \frac{1}{3}\ln\frac{\mu_c^2}{m_c^2}\right)\right)f_+(q^2)\,, \tag{C4}$$

where $E = (m_D^2 - m_P^2 - q^2)/(2m_D)$. In our analysis we interpolate between (C4) and (C3) and take f_0 from a lattice calculation [73]. For the residual form factor we use the z-expansion [26]

$$f_+(q^2) = \frac{1}{\phi(q^2, t_0)}\sum_{i=0}^{\infty} a_i(t_0)\left(z(q^2, t_0)\right)^i\,, \tag{C5}$$

with

$$z(q^2,t_0)=\frac{\sqrt{t_+-q^2}-\sqrt{t_+-t_0}}{\sqrt{t_+-q^2}+\sqrt{t_+-t_0}}\,,\quad t_\pm=(m_D\pm m_P)^2\,,\quad t_0=t_+\left(1-\sqrt{1-\frac{t_-}{t_+}}\right)\,, \tag{C6}$$

$$\phi(q^2,t_0)=\sqrt{\frac{\pi m_c^2}{3}}\left(\sqrt{t_+-q^2}+\sqrt{t_+-t_0}\right)\frac{t_+-q^2}{(t_+-t_0)^{1/4}}\frac{\left(\sqrt{t_+-q^2}+\sqrt{t_+-t_-}\right)^{3/2}}{\left(\sqrt{t_+-q^2}+\sqrt{t_+}\right)^5}\,. \tag{C7}$$

Assuming isospin symmetry, we employ the parameters to second order as given by HFAG [26]

$$f_+(0)\,|V_{cd}|=0.1425\pm0.0019\,,\quad r_1=-1.94\pm0.19\,,\quad r_2=-0.62\pm1.19\,, \tag{C8}$$

where $r_i\equiv a_i/a_0$ and $m_i=(m_{i^+}+m_{i^0})/2$. Lattice computations for $f_+(q^2)$ [73] are consistent with [26], and find insensitivity of f_+ to the spectator quark. We therefore use identical numerics for $D\to\pi$ and $D_s\to K$ form factors. The form factors as used in our analysis are shown in Fig. 5. We do not take into account uncertainties in f_0, which are $\lesssim 10\%$ [73] as this enters BSM predictions only, and because they are negligible in view of other uncertainties.

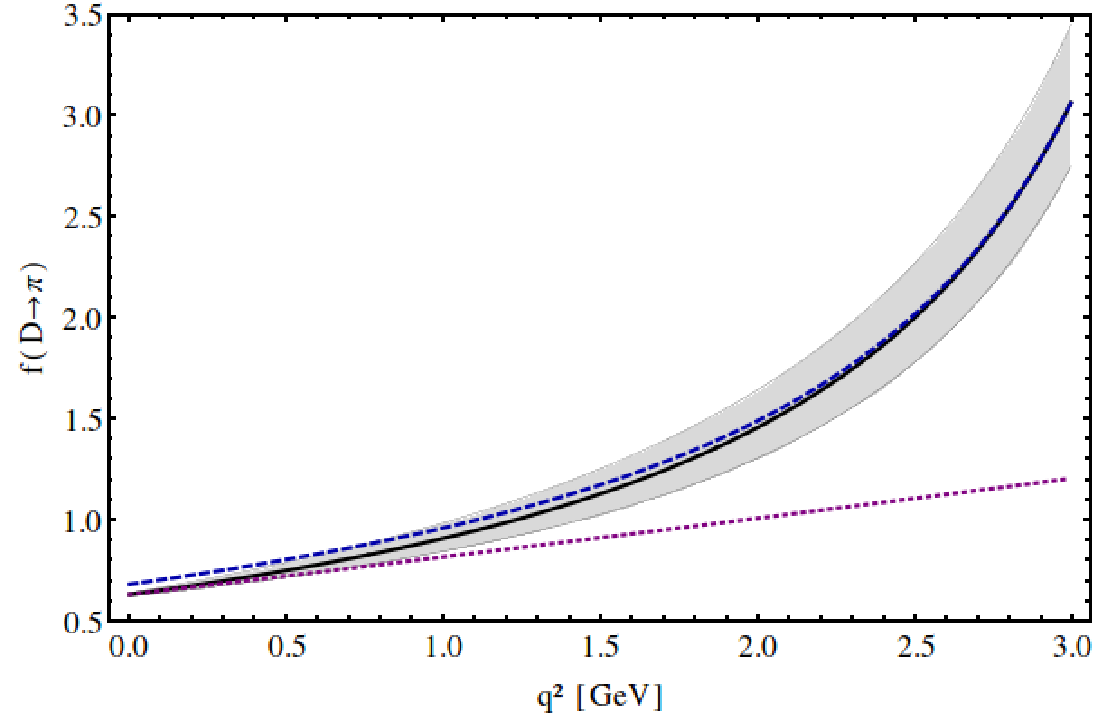

FIG. 5: The solid black line denotes f_+ within its gray uncertainty band, the dashed blue curve denotes $f_T(\mu_c=m_c)$ as derived from Eqs. (C4), (C3) and the dotted purple curve denotes f_0 as calculated on the lattice [73]. Uncertainties for f_T that follow from the parametric ones of f_+ are not shown too avoid clutter, but are included in our analysis.

Appendix D: Exclusive Charm Decay Observables

Here we give the observables for exclusive charm decays used in our analysis. The form factors f_i are defined in App. C. We neglect non-factorizable terms. The $D\to Pll$ distributions are in agreement with [34]. The dilepton spectrum reads

$$
\begin{aligned}
\frac{\mathrm{d}\Gamma}{\mathrm{d}q^2} = \frac{G_F^2\alpha_e^2}{1024\pi^5 m_D^3}\Bigg(\frac{2}{3}\left(\left(|C_9|^2+|C_{10}|^2\right)f_+^2+4|C_7|^2 f_T^2\frac{m_c^2}{m_D^2}+4\mathrm{Re}\left[C_7C_9^*\right]f_Tf_+\frac{m_c}{m_D}\right) \\
\times\lambda(m_D^2,m_P^2,q^2)\left(1+\frac{2m_l^2}{q^2}\right)+|C_{10}|^2\left(-f_+^2\lambda(m_D^2,m_P^2,q^2)+f_0^2\left(m_D^2-m_P^2\right)^2\right)\frac{4m_l^2}{q^2} \\
+\left(|C_S|^2\left(q^2-4m_l^2\right)+|C_P|^2q^2\right)f_0^2\frac{\left(m_D^2-m_P^2\right)^2}{m_c^2} \\
+\frac{4}{3}\left(|C_T|^2+|C_{T5}|^2\right)f_T^2\frac{q^2\lambda(m_D^2,m_P^2,q^2)}{m_D^2}\left(1-\frac{4m_l^2}{q^2}\right) \\
+8\mathrm{Re}\left[\left(C_9f_++2C_7f_T\frac{m_c}{m_D}\right)C_T^*\right]f_T\frac{\lambda(m_D^2,m_P^2,q^2)}{m_D}m_l \\
+4\mathrm{Re}\left[C_{10}C_P^*\right]f_0^2\frac{\left(m_D^2-m_P^2\right)^2}{m_c}m_l \\
+16|C_T|^2f_T^2\frac{\lambda(m_D^2,m_P^2,q^2)}{m_D^2}m_l^2\Bigg)\sqrt{\lambda(m_D^2,m_P^2,q^2)\left(1-\frac{4m_l^2}{q^2}\right)}\,,
\end{aligned}
\tag{D1}
$$

where $\lambda(a,b,c)=a^2+b^2+c^2-2ab-2ac-2bc$. The differential lepton forward-backward asymmetry defined as the asymmetry between forward minus backward flying l^- in the dilepton center of mass frame relative to the recoiling P reads

$$
\begin{aligned}
A_{\mathrm{FB}}(q^2) = N\frac{G_F^2\alpha_e^2}{512\pi^5m_D^3}\Bigg(\mathrm{Re}\left[\left(C_SC_T^*+C_PC_{T5}^*\right)\right]f_T\frac{m_D^2-m_P^2}{m_c\,m_D}q^2 \\
+\mathrm{Re}\left[\left(C_9f_++2C_7f_T\frac{m_c}{m_D}\right)C_S^*\right]\frac{m_D^2-m_P^2}{m_c}m_l \\
+2\mathrm{Re}\left[C_{10}C_{T5}^*\right]f_T\frac{m_D^2-m_P^2}{m_D}m_l\Bigg)f_0\lambda(m_D^2,m_P^2,q^2)\left(1-\frac{4m_l^2}{q^2}\right)\,.
\end{aligned}
\tag{D2}
$$

For vanishing lepton masses the flat term [34] reads

$$
\begin{aligned}
F_H(q^2) = N\frac{G_F^2\alpha_e^2}{2048\pi^5m_D^3}\Bigg(\left(|C_S|^2+|C_P|^2\right)f_0^2\frac{\left(m_D^2-m_P^2\right)^2}{m_c^2} \\
+4\left(|C_T|^2+|C_{T5}|^2\right)f_T^2\frac{\lambda(m_D^2,m_P^2,q^2)}{m_D^2}\Bigg)q^2\sqrt{\lambda(m_D^2,m_P^2,q^2)}+\mathcal{O}(m_l)\,,
\end{aligned}
\tag{D3}
$$

where $N^{-1}=\int_{q^2_{\mathrm{min}}}^{q^2_{\mathrm{max}}}\mathrm{d}q^2\,\mathrm{d}\Gamma/\mathrm{d}q^2$. For the LFV $D\to Pe\mu$ decay distributions we obtain, for $m_e=0$,

$$
\begin{aligned}
\frac{\mathrm{d}\Gamma(D^+\to P^+e^\pm\mu^\mp)}{\mathrm{d}q^2} = \frac{G_F^2\alpha_e^2}{1024\pi^5m_D^3}\sqrt{\lambda(m_D^2,m_P^2,q^2)}\Bigg(\frac{2}{3}\left(|K_9|^2+|K_{10}|^2\right)f_+^2\lambda(m_D^2,m_P^2,q^2) \\
+\left(|K_S|^2+|K_P|^2\right)f_0^2\frac{\left(m_D^2-m_P^2\right)^2}{m_c^2}q^2 \\
+\frac{4}{3}\left(|K_T|^2+|K_{T5}|^2\right)f_T^2\frac{q^2\lambda(m_D^2,m_P^2,q^2)}{m_D^2} \\
+2\mathrm{Re}\left[\pm K_9K_S^*+K_{10}K_P^*\right]f_0^2\frac{\left(m_D^2-m_P^2\right)^2}{m_c}m_\mu \\
+4\mathrm{Re}\left[K_9K_T^*\pm K_{10}K_{T5}^*\right]f_Tf_+\frac{\lambda(m_D^2,m_P^2,q^2)}{m_D}m_\mu\Bigg)+\mathcal{O}\left(m_\mu^2\right)\,,
\end{aligned}
\tag{D4}
$$

where $K_i=K_i^{(\mu)}$ and the plus signs for $D^+\to P^+e^+\mu^-$, and $K_i=K_i^{(e)}$ and the minus signs for $D^+\to P^+e^+\mu^-$. Compared to Eq. (D1), additional vector-scalar and axialvector-axialtensor are present in Eq. (D4).

All Wilson coefficients except for those of the tensors in Eqs. (D1)-(D4) are tacitly understood as $C_i \to C_i + C_i'$ and $K_i \to K_i + K_i'$, that is, primed Wilson coefficients are added.

The $D^0 \to l^+l^-$ branching fraction can be inferred from [34]

$$\mathcal{B}(D^0 \to l^+l^-) = \frac{G_F^2 \alpha_e^2 m_{D^0}^5 f_{D^0}^2}{64\pi^3 \Gamma_{D^0}} \sqrt{1 - \frac{4m_l^2}{m_{D^0}^2}} \left(\left(1 - \frac{4m_l^2}{m_{D^0}^2}\right) \left| \frac{C_S - C_S'}{m_c} \right|^2 + \left| \frac{C_P - C_P'}{m_c} + \frac{2m_l}{m_{D^0}^2}(C_{10} - C_{10}') \right|^2 \right). \tag{D5}$$

The LFV ones read, for $m_e = 0$,

$$\begin{aligned}
\mathcal{B}(D^0 \to e^-\mu^+) &= \frac{G_F^2 \alpha_e^2 m_{D^0}^5 f_{D^0}^2}{64\pi^3 \Gamma_{D^0}} \left(1 - \frac{m_\mu^2}{m_{D^0}^2}\right)^2 \left(\left| \frac{K_S^{(e)} - K_S^{(e)\prime}}{m_c} - \frac{m_\mu}{m_{D^0}^2}\left(K_9^{(e)} - K_9^{(e)\prime}\right) \right|^2 \right. \\
&\quad \left. + \left| \frac{K_P^{(e)} - K_P^{(e)\prime}}{m_c} + \frac{m_\mu}{m_{D^0}^2}\left(K_{10}^{(e)} - K_{10}^{(e)\prime}\right) \right|^2 \right), \\
\mathcal{B}(D^0 \to \mu^-e^+) &= \frac{G_F^2 \alpha_e^2 m_{D^0}^5 f_{D^0}^2}{64\pi^3 \Gamma_{D^0}} \left(1 - \frac{m_\mu^2}{m_{D^0}^2}\right)^2 \left(\left| \frac{K_S^{(\mu)} - K_S^{(\mu)\prime}}{m_c} + \frac{m_\mu}{m_{D^0}^2}\left(K_9^{(\mu)} - K_9^{(\mu)\prime}\right) \right|^2 \right. \\
&\quad \left. + \left| \frac{K_P^{(\mu)} - K_P^{(\mu)\prime}}{m_c} + \frac{m_\mu}{m_{D^0}^2}\left(K_{10}^{(\mu)} - K_{10}^{(\mu)\prime}\right) \right|^2 \right).
\end{aligned} \tag{D6}$$

Appendix E: Non-resonant SM $c \to ull$ Branching Fractions

In this appendix we provide our predictions for the non-resonant SM branching fractions of the inclusive $c \to ull$ decays and exclusive $D \to Pll$ modes. In our analysis uncertainties due to power corrections are not included. Electroweak corrections, which are subleading relative to QCD-ones, are neglected. For the $D \to Pll$ modes we integrate the branching fractions over different dilepton masses, $\sqrt{q^2} \geq 2m_l$ (Table VIII), $0.250\,\text{GeV} \leq \sqrt{q^2} \leq 0.525\,\text{GeV}$ (Table IX) and $\sqrt{q^2} \geq 1.25\,\text{GeV}$ (Table X).

mode	branching fraction	90% CL limit [31]
$D^+ \to \pi^+ e^+ e^-$	$4.6 \cdot 10^{-12}\,(\pm 1, {}^{+2}_{-1}, {}^{+14}_{-13}, \pm 1, {}^{+5}_{-1}, {}^{+210}_{-3}, {}^{+13}_{-10})$	$1.1 \cdot 10^{-6}$
$D^+ \to \pi^+ \mu^+ \mu^-$	$3.7 \cdot 10^{-12}\,(\pm 1, \pm 3, {}^{+16}_{-15}, \pm 1, {}^{+3}_{-1}, {}^{+158}_{-1}, {}^{+16}_{-12})$	$7.3 \cdot 10^{-8}$
$D^0 \to \pi^0 e^+ e^-$	$9.1 \cdot 10^{-13}\,(\pm 1, \pm 1, {}^{+14}_{-13}, \pm 1, {}^{+5}_{-1}, {}^{+211}_{-2}, {}^{+13}_{-10})$	$4.5 \cdot 10^{-5}$
$D^0 \to \pi^0 \mu^+ \mu^-$	$7.3 \cdot 10^{-13}\,(\pm 1, \pm 3, {}^{+16}_{-15}, \pm 1, {}^{+3}_{-1}, {}^{+159}_{-1}, {}^{+16}_{-12})$	$1.8 \cdot 10^{-4}$
$D_s^+ \to K^+ e^+ e^-$	$1.7 \cdot 10^{-12}\,(\pm 2, {}^{+4}_{-3}, {}^{+13}_{-12}, {}^{+7}_{-1}, {}^{+8}_{-1}, {}^{+228}_{-7}, {}^{+10}_{-8})$	$3.7 \cdot 10^{-6}$
$D_s^+ \to K^+ \mu^+ \mu^-$	$1.2 \cdot 10^{-12}\,(\pm 2, {}^{+2}_{-1}, {}^{+16}_{-15}, \pm 2, {}^{+4}_{-1}, {}^{+167}_{-1}, {}^{+13}_{-10})$	$2.1 \cdot 10^{-5}$

TABLE VIII: Non-resonant SM branching fractions for $\sqrt{q^2} \geq 2m_l$ of $D \to Pll$ decays normalized to the width. Non-negligible uncertainties are labeled by (normalization, m_c, m_s, μ_W, μ_b, μ_c, f_+) given in percentage, where $m_{W,b}/2 \leq \mu_{W,b} \leq 2m_{W,b}$ and $m_c/\sqrt{2} \leq \mu_c \leq \sqrt{2}m_c$.

Next, we obtain inclusive $c \to ull$ branching fractions. To leading order in the heavy quark expansion and neglecting lepton masses the q^2-distribution reads [74]

$$\frac{\mathrm{d}\Gamma(c \to ull)}{\mathrm{d}q^2} = \frac{G_F^2 \alpha_e^2 m_c^3}{768\pi^5} \left(1 - \frac{q^2}{m_c^2}\right)^2 \left[\left(1 + 2\frac{q^2}{m_c^2}\right)\left(|C_9|^2 + |C_{10}|^2\right) + 4\left(2\frac{m_c^2}{q^2} + 1\right)|C_7|^2 + 12\mathrm{Re}\left[C_7 C_9^*\right] \right], \tag{E1}$$

where $q^2 = (p_c - p_u)^2 = (p_{l^+} + p_{l^-})^2$ and $(2m_l)^2 \leq q^2 \leq m_c^2$.

mode	branching fraction	90% CL limit [30]
$D^+ \to \pi^+ e^+ e^-$	$8.1 \cdot 10^{-13}\,(\pm 1, ^{+5}_{-4}, ^{+23}_{-22}, ^{+11}_{-12}, ^{+10}_{-1}, ^{+247}_{-24}, \pm 5)$	–
$D^+ \to \pi^+ \mu^+ \mu^-$	$7.4 \cdot 10^{-13}\,(\pm 1, \pm 4, ^{+23}_{-21}, ^{+10}_{-11}, ^{+10}_{-1}, ^{+238}_{-23}, ^{+6}_{-5})$	$2.0 \cdot 10^{-8}$
$D^0 \to \pi^0 e^+ e^-$	$1.6 \cdot 10^{-13}\,(\pm 1, ^{+5}_{-4}, ^{+23}_{-22}, ^{+11}_{-12}, ^{+10}_{-1}, ^{+247}_{-24}, \pm 5)$	–
$D^0 \to \pi^0 \mu^+ \mu^-$	$1.5 \cdot 10^{-13}\,(\pm 1, \pm 4, ^{+23}_{-21}, ^{+10}_{-11}, ^{+10}_{-1}, ^{+238}_{-22}, ^{+6}_{-5})$	–
$D_s^+ \to K^+ e^+ e^-$	$3.6 \cdot 10^{-13}\,(\pm 2, \pm 5, ^{+23}_{-22}, ^{+12}_{-13}, ^{+11}_{-1}, ^{+248}_{-21}, \pm 5)$	–
$D_s^+ \to K^+ \mu^+ \mu^-$	$3.3 \cdot 10^{-13}\,(\pm 2, \pm 5, ^{+23}_{-22}, ^{+12}_{-13}, ^{+11}_{-1}, ^{+239}_{-20}, ^{+6}_{-5})$	–

TABLE IX: As in Table VIII but for the low q^2-region, $0.250\,\mathrm{GeV} \leq \sqrt{q^2} \leq 0.525\,\mathrm{GeV}$.

mode	branching fraction	90% CL limit [30]
$D^+ \to \pi^+ l^+ l^-$	$7.4 \cdot 10^{-13}\,(\pm 1, \pm 6, ^{+15}_{-14}, \pm 6, ^{+0}_{-1}, ^{+136}_{-45}, ^{+27}_{-20})$	$2.6 \cdot 10^{-8}\ (l = \mu)$
$D^0 \to \pi^0 l^+ l^-$	$1.4 \cdot 10^{-13}\,(\pm 1, \pm 6, ^{+15}_{-14}, \pm 6, ^{+0}_{-1}, ^{+136}_{-45}, ^{+27}_{-20})$	–
$D_s^+ \to K^+ l^+ l^-$	$7.9 \cdot 10^{-14}\,(\pm 2, \pm 6, ^{+15}_{-14}, \pm 6, ^{+0}_{-1}, ^{+133}_{-45}, ^{+26}_{-19})$	–

TABLE X: As in Table VIII but for the high q^2-region, $\sqrt{q^2} \geq 1.25\,\mathrm{GeV}$, and $l = e, \mu$.

The matrix elements at NLO QCD are obtained as $C_i \to C_i(1 + \alpha_s/\pi\, \sigma_i(q^2/m_c^2))$ [75] (and references therein)

$$\sigma_7(\rho) = -\frac{4}{3}\mathrm{Li}_2[\rho] - \frac{2}{3}\ln\rho\ln[1-\rho] - \frac{2}{9}\pi^2 - \ln[1-\rho] - \frac{2}{9}(1-\rho)\ln[1-\rho] + \frac{1}{6} - \frac{4}{3}\ln\frac{\mu_c^2}{m_c^2}\,, \tag{E2}$$

$$\sigma_9(\rho) = -\frac{4}{3}\mathrm{Li}_2[\rho] - \frac{2}{3}\ln\rho\ln[1-\rho] - \frac{2}{9}\pi^2 - \ln[1-\rho] - \frac{2}{9}(1-\rho)\ln[1-\rho] + \frac{3}{2}\,, \tag{E3}$$

where $\sigma_{10} = \sigma_9$ and via $\mathrm{Re}[C_i C_j^*] \to \mathrm{Re}[C_i C_j^*](1 + \alpha_s/\pi\, \tau_{ij}^{(1)}(q^2/m_c^2))$

$$\tau_{77}^{(1)}(\rho) = -\frac{2}{9(2+\rho)}\left(2(1-\rho)^2\ln[1-\rho] + \frac{6\rho(2-2\rho-\rho^2)}{(1-\rho)^2}\ln\rho + \frac{11-7\rho-10\rho^2}{1-\rho}\right)\,, \tag{E4}$$

$$\tau_{99}^{(1)}(\rho) = -\frac{4}{9(1+2\rho)}\left(2(1-\rho)^2\ln[1-\rho] + \frac{3\rho(1+\rho)(1-2\rho)}{(1-\rho)^2}\ln\rho + \frac{3(1-3\rho^2)}{1-\rho}\right)\,, \tag{E5}$$

$$\tau_{79}^{(1)}(\rho) = -\frac{4(1-\rho)^2}{9\rho}\ln[1-\rho] - \frac{4\rho(3-2\rho)}{9(1-\rho)^2}\ln\rho - \frac{2(5-3\rho)}{9(1-\rho)}\,, \tag{E6}$$

$$\begin{aligned}\tau_{710}^{(1)}(\rho) = &-\frac{5}{2} + \frac{1}{3(1-3\rho)} - \frac{\rho(6-7\rho)\ln\rho}{3(1-\rho)^2} - \frac{(3-7\rho+4\rho^2)\ln[1-\rho]}{9\rho} \\ &+ \frac{1}{18(1-\rho)^2}\big[24\left(1+13\rho-4\rho^2\right)\mathrm{Li}_2[\sqrt{\rho}] + 12\left(1-17\rho+6\rho^2\right)\mathrm{Li}_2[\rho] + 6\rho(6-7\rho)\ln\rho \\ &+ 24(1-\rho)^2\ln\rho\ln[1-\rho] + 12\left(-13+16\rho-3\rho^2\right)(\ln[1-\sqrt{\rho}] - \ln[1-\rho]) \\ &+ 39 - 2\pi^2 + 252\rho - 26\pi^2\rho + 21\rho^2 + 8\pi^2\rho^2 - 180\sqrt{\rho} - 132\rho\sqrt{\rho}\big]\,,\end{aligned} \tag{E7}$$

$$\begin{aligned}\tau_{910}^{(1)}(\rho) = &-\frac{5}{2} + \frac{1}{3(1-\rho)} - \frac{\rho(6-7\rho)\ln\rho}{3(1-\rho)^2} - \frac{2(3-5\rho+2\rho^2)\ln[1-\rho]}{9\rho} \\ &- \frac{1}{18(1-\rho)^2}\big[48\rho(-5+2\rho)\mathrm{Li}_2[\sqrt{\rho}] + 24\left(-1+7\rho-3\rho^2\right)\mathrm{Li}_2[\rho] + 6\rho(-6+7\rho)\ln\rho \\ &- 24(1-\rho)^2\ln\rho\ln[1-\rho] + 24\left(5-7\rho+2\rho^2\right)(\ln[1-\sqrt{\rho}] - \ln[1-\rho]) \\ &- 21 - 156\rho + 20\pi^2\rho + 9\rho^2 - 8\pi^2\rho^2 + 120\sqrt{\rho} + 48\rho\sqrt{\rho}\big]\,,\end{aligned} \tag{E8}$$

where $\tau_{10\,10} = \tau_{99}$. We obtain the NNLO term $\delta^{(2)}|C_9|^2 = |C_9|^2(\alpha_s/\pi)^2\,\tau_{99}^{(2)}(q^2/m_c^2)$ as [76]

$$\begin{aligned}\tau_{99}^{(2)}(\rho) = \frac{1}{(1-\rho)^2\,(1+2\rho)}\Big[&2\left(2.854 - 0.665\rho - 0.109\rho^2 - 8.572\rho^3 + 5.561\rho^4 + 0.931\rho^5\right)\\ &+ \frac{2}{3}\left(-0.063615 + 0.098146\rho + 0.144642\rho^2 - 0.307331\rho^3 + 0.107417\rho^4 + 0.020707\rho^5\right)\\ &+ \frac{16}{9}\left(3.575 - 2.867\rho + 2.241\rho^2 - 12.027\rho^3 + 11.564\rho^4 - 2.489\rho^5\right)\\ &+ 4\left(-8.151 + 2.990\rho - 3.537\rho^2 + 36.561\rho^3 - 42.275\rho^4 + 23.899\rho^5 - 9.494\rho^6\right)\Big]\,. \end{aligned} \tag{E9}$$

We normalize to the $c \to (d,s)l\nu$ width and the experimental branching fraction

$$\frac{\mathrm{d}\mathcal{B}_{D\to X_u ll}}{\mathrm{d}q^2} = \frac{\mathcal{B}(D \to X_{(d,s)}l\nu)}{\Gamma_{c\to(d,s)l\nu}}\frac{\mathrm{d}\Gamma_{c\to ull}}{\mathrm{d}q^2} \tag{E10}$$

with [77]

$$\Gamma_{c\to(d,s)l\nu} = \frac{G_F^2 m_c^3}{192\pi^3}\sum_{q\in\{d,s\}}|V_{cq}|^2\left(X_0(m_q/m_c) + \frac{\alpha_s}{\pi}X_1(m_q/m_c) + \left(\frac{\alpha_s}{\pi}\right)^2 X_2(m_q/m_c)\right)\,, \tag{E11}$$

where the functions X_i are given in [77]. Power corrections can be inferred from [78, 79]. They are, however, not included in our numerical analysis, as the OPE breaks down for large q^2 when the inclusive decay ceases to be inclusive but rather degenerates into few exclusive modes. Yet, the power corrections in the region where the OPE works are a small effect on the uncertainty budget at low q^2. A comprehensive treatment of the full q^2-region is beyond the scope of this work. Our resulting inclusive $c \to ull$ branching fractions are compiled in Table XI.

mode	branching fraction
$D^+ \to X_u^+ e^+ e^-$	$9.4 \cdot 10^{-10}\,(\pm 2, {}^{+7}_{-6}, {}^{+16}_{-14}, \pm 7, \pm 1, {}^{+109}_{-43})$
$D^+ \to X_u^+ \mu^+ \mu^-$	$2.0 \cdot 10^{-10}\,(\pm 19, {}^{+5}_{-5}, {}^{+15}_{-14}, {}^{+8}_{-7}, \pm 1, {}^{+120}_{-40})$
$D^0 \to X_u^0 e^+ e^-$	$3.8 \cdot 10^{-10}\,(\pm 2, {}^{+7}_{-6}, {}^{+16}_{-14}, \pm 7, \pm 1, {}^{+109}_{-43})$
$D^0 \to X_u^0 \mu^+ \mu^-$	$7.7 \cdot 10^{-11}\,(\pm 9, {}^{+5}_{-5}, {}^{+15}_{-14}, {}^{+8}_{-7}, \pm 1, {}^{+120}_{-40})$
$D_s^+ \to X_u^+ e^+ e^-$	$3.8 \cdot 10^{-10}\,(\pm 7, {}^{+7}_{-6}, {}^{+16}_{-14}, \pm 7, \pm 1, {}^{+109}_{-43})$
$D_s^+ \to X_u^+ \mu^+ \mu^-$	$7.5 \cdot 10^{-11}\,(\pm 7, {}^{+5}_{-5}, {}^{+15}_{-14}, {}^{+8}_{-7}, \pm 1, {}^{+120}_{-40})$

TABLE XI: Non-resonant SM branching fractions for $\sqrt{q^2} \geq 2m_l$ of $D \to X_u ll$ decays normalized to $D \to X_{d,s}l\nu$ and vanishing lepton masses except for the lower cut. Non-negligible uncertainties are labeled by (normalization, m_c, m_s, μ_W, μ_b, μ_c) given in percentage, where $m_{W,b}/2 \leq \mu_{W,b} \leq 2m_{W,b}$ and $m_c/\sqrt{2} \leq \mu_c \leq \sqrt{2}m_c$.

Appendix F: Leptoquark Constraints

In this appendix we provide constraints on the couplings of the scalar and vector leptoquarks of Table III. Collider experiments find $M \gtrsim 1$ TeV [80, 81], thus we use $M = 1\,\mathrm{TeV}$ as reference. We neglect RGE effects from M to μ_W and further to μ_c noting that Q_9 and Q_{10} do not scale and $C_{S,P}(\mu \sim 1\,\mathrm{TeV}) \simeq 0.5\,C_{S,P}(\mu \sim \mu_c)$ and $C_{T,T5}(\mu \sim 1\,\mathrm{TeV}) \simeq 1.3\,C_{T,T5}(\mu \sim \mu_c)$ at one-loop QCD [34]. Neglecting such effects is within the accuracy aimed at in this work. We do not constrain non-gauge vector leptoquarks, which could depend on the cutoff-scale within some model [45]. We first list the constraints on the couplings and the related observables for scalar (Tables XII and XIII) and vector (Table XIV) leptoquarks. Our constraints are consistent with, update and extend those of [45, 54] and we note that quark doublet couplings are additionally constrained by kaon physics [45, 54]. Results are given in Table XV. Next, we calculate the constraints of Tables XII-XIV, where the experimental limits are given in App. A. We note that fermion doublets coupling to leptoquarks are implicitly added. We obtain constraints using $D \to Pll$ (Eq. (D1)), $D \to Pe\mu$ (Eq. (D4)), $D \to ll$ (Eq. (D5)) and $D \to \mu e$ (Eq. (D6)).

Scalar leptoquarks contribute to the $D^0 - \bar{D}^0$ mass difference [45, 82]

$$\Delta^S m_{D^0} = \frac{2}{3}m_D f_D^2 B_D \frac{\left(\lambda_{L,R}^{(cl)}\left(\lambda_{L,R}^{(ul)}\right)^*\right)^2}{64\pi^2 M^2} \tag{F1}$$

couplings/mass	constraint	observable
$\lvert\lambda^{(ue)}_{S_1 L}\rvert$	$\lesssim 9\cdot 10^{-2}$	V_{ud}
$\lambda^{(ue)}_L \lambda^{(ue)}_R$	$\sim [-0.08, 0.8]$	nuclear beta decay
$\lvert\lambda^{(ue)}_L \lambda^{(u\mu)}_R\rvert$	$\lesssim 9\cdot 10^{-2}$	$\pi^+ \to \mu^+ \nu_e$
$\lvert\lambda^{(ue)}_{\{L,R\}} \lambda^{(ce)}_{\{L,R\}}\rvert$	$\lesssim 1\cdot 10^{-1}$	$D^+ \to \pi^+ e^+ e^-$
$\lvert\lambda^{(ue)}_{\{L,R\}} \lambda^{(c\mu)}_{\{L,R\}}\rvert$	$\lesssim 2\cdot 10^{-1}$	$D^+ \to \pi^+ e^+ \mu^-$
$\lvert\lambda^{(u\mu)}_{\{L,R\}} \lambda^{(ce)}_{\{L,R\}}\rvert$	$\lesssim 2\cdot 10^{-1}$	$D^+ \to \pi^+ e^- \mu^+$
$\lvert\lambda^{(u\mu)}_{\{L,R\}} \lambda^{(c\mu)}_{\{L,R\}}\rvert$	$\lesssim 2\cdot 10^{-2}$	$D^+ \to \pi^+ \mu^+ \mu^-$
$\lambda^{(ce)}_L \lambda^{(ce)}_R$	$\sim [-0.005, 0.05]$	$D_s^+ \to \mu^+ \nu_\mu$
$\lambda^{(ce)}_L \lambda^{(ce)}_R$	$\sim [0.00, 0.01]$	Δa_e
$\lambda^{(c\mu)}_L \lambda^{(c\mu)}_R$	$\sim [-0.2, -0.1]$	Δa_μ
$(-\lvert\lambda^{(ue)}_{S_1 L, S_2 L}\rvert^2 + \lvert\lambda^{(ue)}_{S_1 R, S_2 R}\rvert^2 + \lvert\lambda^{(ue)}_{S_2 R}\rvert^2)^{1/2}$	$\sim [0.2, 0.4]$	$Q_w\,(\mathrm{Cs})$
$(\lambda^{(ue)}_L \lambda^{(ue)}_R - 0.02\,\lambda^{(u\mu)}_L \lambda^{(u\mu)}_R$ $-0.0002\,(\lvert\lambda^{(ue)}_{S_1 L}\rvert^2 - \lvert\lambda^{(u\mu)}_{S_1 L}\rvert^2))$	$\sim [-0.00001, -0.000003]$	$\Delta R_{e/\mu}$
$(\lambda^{(ue)}_{S_1 L, S_2 R} \lambda^{(ce)}_{S_1 R, S_2 L} - 0.02\,\lambda^{(ue)}_{S_1 L} \lambda^{(ce)}_{S_1 L})$	$\sim [-0.009, 0.01]$	$D^+ \to \mu^+ \nu_\mu$
$\lvert\lambda^{(ue)}_L \lambda^{(ce)}_R \pm \lambda^{(ue)}_R \lambda^{(ce)}_L\rvert$	$\lesssim 1\cdot 10^{-2}$	$D^0 \to e^+ e^-$
$\lambda^{(ue)}_{L,R} \lambda^{(ce)}_{L,R} + \lambda^{(u\mu)}_{L,R} \lambda^{(c\mu)}_{L,R}$	$\sim [0, 0.01]$	Δm_{D^0}
$\lvert\lambda^{(qe)}_{S_1 L, S_1 R} \lambda^{(q\mu)}_{S_1 L, S_1 R}\rvert$	$\lesssim 1\cdot 10^{-3}$	$\mu^- \to e^- \gamma$
$\lvert\lambda^{(qe)}_{S_2 L, S_2 R} \lambda^{(q\mu)}_{S_2 L, S_2 R}\rvert$	$\lesssim 5\cdot 10^{-4}$	
$\lvert\lambda^{(ce)}_{L,R} \lambda^{(c\mu)}_{R,L}\rvert$	$\lesssim 3\cdot 10^{-6}$	
$\lvert\lambda^{(ue)}_{L,R} \lambda^{(u\mu)}_{L,R}\rvert$	$\lesssim 9\cdot 10^{-7}$	$\mu - e\,(\mathrm{Au})$
$\lvert\lambda^{(ue)}_{S_2 R} \lambda^{(u\mu)}_{S_2 R}\rvert$	$\lesssim 7\cdot 10^{-7}$	
$\lvert\lambda^{(ue)}_{L,R} \lambda^{(u\mu)}_{R,L}\rvert$	$\lesssim 4\cdot 10^{-7}$	
$\lvert\lambda^{(ce)}_{S_1 L, S_1 R} \lambda^{(c\mu)}_{S_1 L, S_1 R}\rvert$	$\lesssim 9\cdot 10^{-3}$	
$\lvert\lambda^{(ce)}_{S_2 L, S_2 R} \lambda^{(c\mu)}_{S_2 L, S_2 R}\rvert$	$\lesssim 3\cdot 10^{-3}$	
$\lvert\lambda^{(ce)}_{L,R} \lambda^{(c\mu)}_{R,L}\rvert$	$\lesssim 1\cdot 10^{-5}$	
$\lvert\lambda^{(ue)}_{L,R} \lambda^{(u\mu)}_{L,R}\rvert$	$\lesssim 1\cdot 10^{-3}$	$\mu^- \to e^- e^+ e^-$
$\lvert\lambda^{(ue)}_{S_2 R} \lambda^{(u\mu)}_{S_2 R}\rvert$	$\lesssim 3\cdot 10^{-3}$	
$\lvert\lambda^{(ue)}_{L,R} \lambda^{(u\mu)}_{R,L}\rvert$	$\lesssim 1\cdot 10^{-2}$	
$\lvert\lambda^{(ce)}_{L,R} \lambda^{(c\mu)}_{L,R}\rvert$	$\lesssim 3\cdot 10^{-3}$	
$\lvert\lambda^{(ce)}_{S_2 R} \lambda^{(c\mu)}_{S_2 R}\rvert$	$\lesssim 6\cdot 10^{-3}$	
$\lvert\lambda^{(ce)}_{S_1 L, S_1 R} \lambda^{(c\mu)}_{S_1 R, S_1 L}\rvert$	$\lesssim 6\cdot 10^{-5}$	
$\lvert\lambda^{(ce)}_{S_2 L, S_2 R} \lambda^{(c\mu)}_{S_2 R, S_2 L}\rvert$	$\lesssim 5\cdot 10^{-5}$	
$\lvert\lambda^{(ue)}_{L,R} \lambda^{(c\mu)}_{L,R} + \lambda^{(u\mu)}_{L,R} \lambda^{(ce)}_{L,R}\rvert$	$\lesssim 8\cdot 10^{-1}$	$D^0 \to \mu^\pm e^\mp$
$\lvert\lambda^{(ue)}_{L,R} \lambda^{(c\mu)}_{R,L} + \lambda^{(u\mu)}_{L,R} \lambda^{(ce)}_{R,L}\rvert$	$\lesssim 1\cdot 10^{-2}$	
$\lvert\lambda^{(u\mu)}_L \lambda^{(c\mu)}_L + \lambda^{(u\mu)}_R \lambda^{(c\mu)}_R\rvert$	$\lesssim 6\cdot 10^{-2}$	$D^0 \to \mu^+ \mu^-$
$\lvert\lambda^{(u\mu)}_L \lambda^{(c\mu)}_R \pm \lambda^{(u\mu)}_R \lambda^{(c\mu)}_L\rvert$	$\lesssim 4\cdot 10^{-3}$	

TABLE XII: Scalar $SU(2)$-singlet and -doublet leptoquark constraints for real couplings scaling as TeV/M and $\sqrt{\mathrm{TeV}/M}$ for Δm_{D^0}. Additionally, $\lvert\mathrm{Im}[\lambda^{(u\mu)}_L (\lambda^{(u\mu)}_R)^*]\rvert \lesssim 3\cdot 10^{-7}$ and $\mathrm{Im}[\lambda^{(ce)}_L (\lambda^{(ce)}_R)^*] \lesssim 3\cdot 10^{-10}$ from bounds on neutron and electron electric dipole moments.

(times 2 for $S_2|_L$ and times 5 for S_3). While constraints from $|\Delta C| = 1$ transitions scale as $\lambda\lambda^*/M^2$, the ones from mixing behave differently, as $(\lambda\lambda^*)^2/M^2$. In our analysis we neglect the SM contribution [83, 84].

Matching onto the nuclear weak charge [85]

$$Q_w(Z,N) = -2((2Z+N)C_{1u} + (2N+Z)C_{1d})\,, \tag{F2}$$

couplings/mass	constraint	observable
$\lvert\lambda^{(ue)}\rvert$	$\lesssim 0.1$	Q_w (Cs)
$\lvert\lambda^{(ue)}\rvert$	$\lesssim 9\cdot 10^{-2}$	V_{ud}
$\lambda^{(ue)}\lambda^{(ce)}$	$\sim [-0.6, 1]$	$D^+ \to \mu^+\nu_\mu$
$\lvert\lambda^{(ue)}\lambda^{(ce)}\rvert$	$\lesssim 1\cdot 10^{-1}$	$D^+ \to \pi^+ e^+ e^-$
$\lvert\lambda^{(ue)}\lambda^{(c\mu)}\rvert$	$\lesssim 2\cdot 10^{-1}$	$D^+ \to \pi^+ e^+ \mu^-$
$\lvert\lambda^{(u\mu)}\lambda^{(ce)}\rvert$	$\lesssim 3\cdot 10^{-1}$	$D^+ \to \pi^+ e^- \mu^+$
$\lvert\lambda^{(u\mu)}\lambda^{(c\mu)}\rvert$	$\lesssim 1\cdot 10^{-2}$	$D^+ \to \pi^+ \mu^+ \mu^-$
$\lvert\lambda^{(u\mu)}\lambda^{(c\mu)}\rvert$	$\lesssim 6\cdot 10^{-2}$	$D^0 \to \mu^+ \mu^-$
$(-\lvert\lambda^{(ue)}\rvert^2 + \lvert\lambda^{(u\mu)}\rvert^2)^{1/2}$	$\sim [0.2, 0.4]$	$\Delta R_{e/\mu}$
$\lvert\lambda^{(ue)}\lambda^{(u\mu)} + \lambda^{(ce)}\lambda^{(c\mu)}\rvert$	$\lesssim 5\cdot 10^{-4}$	$\mu^- \to e^-\gamma$
$(\lambda^{(ue)}\lambda^{(ce)} + \lambda^{(u\mu)}\lambda^{(c\mu)})$	$\sim [0, 0.007]$	Δm_{D^0}
$\lvert\lambda^{(ue)}\lambda^{(c\mu)} + \lambda^{(u\mu)}\lambda^{(ce)}\rvert$	$\lesssim 8\cdot 10^{-1}$	$D^0 \to \mu^\pm e^\mp$
$\lvert\lambda^{(ue)}\lambda^{(u\mu)}\rvert$	$\lesssim 7\cdot 10^{-7}$	$\mu - e$ (Au)
$\lvert\lambda^{(ce)}\lambda^{(c\mu)}\rvert$	$\lesssim 9\cdot 10^{-3}$	
$\lvert\lambda^{(ue)}\lambda^{(u\mu)}\rvert$	$\lesssim 1\cdot 10^{-2}$	$\mu^- \to e^- e^+ e^-$
$\lvert\lambda^{(ce)}\lambda^{(c\mu)}\rvert$	$\lesssim 6\cdot 10^{-3}$	

TABLE XIII: Scalar $SU(2)$-triplet leptoquark constraints for real couplings scaling as TeV$/M$ and $\sqrt{\mathrm{TeV}/M}$ for Δm_{D^0}. For the constraint from the weak charge we apply its 2σ interval.

couplings/mass	constraint	observable
$\lvert\lambda^{(ue)}_{\tilde V_{1,2}}\rvert$	$\lesssim 0.1$	Q_w (Cs)
$\lvert\lambda^{(ue)}_{V_3}\rvert$	~ 0.1	
$\lvert\lambda^{(ue)}_{V_3}\rvert$	$\lesssim 6\cdot 10^{-2}$	V_{ud}
$\lambda^{(ue)}_{V_3}\lambda^{(ce)}_{V_3}$	$\sim [-0.3, 0.5]$	$D^+ \to \mu^+\nu_\mu$
$\lvert\lambda^{(ue)}\lambda^{(ce)}\rvert$	$\lesssim 6\cdot 10^{-2}$	$D^+ \to \pi^+ e^+ e^-$
$\lvert\lambda^{(ue)}\lambda^{(c\mu)}\rvert$	$\lesssim 1\cdot 10^{-1}$	$D^+ \to \pi^+ e^+ \mu^-$
$\lvert\lambda^{(u\mu)}\lambda^{(ce)}\rvert$	$\lesssim 1\cdot 10^{-1}$	$D^+ \to \pi^+ e^- \mu^+$
$\lvert\lambda^{(u\mu)}\lambda^{(c\mu)}\rvert$	$\lesssim 1\cdot 10^{-2}$	$D^+ \to \pi^+ \mu^+ \mu^-$
$\lvert\lambda^{(u\mu)}\lambda^{(c\mu)}\rvert$	$\lesssim 3\cdot 10^{-2}$	$D^0 \to \mu^+ \mu^-$
$(-\lvert\lambda^{(ue)}_{V_3}\rvert^2 + \lvert\lambda^{(u\mu)}_{V_3}\rvert^2)^{1/2}$	$\sim [0.2, 0.3]$	$\Delta R_{e/\mu}$
$\lvert\lambda^{(ue)}\lambda^{(c\mu)} + \lambda^{(u\mu)}\lambda^{(ce)}\rvert$	$\lesssim 4\cdot 10^{-1}$	$D^0 \to \mu^\pm e^\mp$
$\lvert\lambda^{(qe)}\lambda^{(q\mu)}\rvert$	$\lesssim 1\cdot 10^{-4}$	$\mu^- \to e^-\gamma$
$\lvert\lambda^{(qe)}_{V_3}\lambda^{(q\mu)}_{V_3}\rvert$	$\lesssim 6\cdot 10^{-5}$	
$\lvert\lambda^{(ue)}\lambda^{(u\mu)}\rvert$	$\lesssim 7\cdot 10^{-7}$	$\mu - e$ (Au)
$\lvert\lambda^{(ce)}_{\tilde V_1,\tilde V_2}\lambda^{(c\mu)}_{\tilde V_1,\tilde V_2}\rvert$	$\lesssim 1\cdot 10^{-2}$	
$\lvert\lambda^{(ce)}_{V_2}\lambda^{(c\mu)}_{V_2}\rvert$	$\lesssim 6\cdot 10^{-3}$	
$\lvert\lambda^{(ce)}_{V_3}\lambda^{(c\mu)}_{V_3}\rvert$	$\lesssim 7\cdot 10^{-3}$	
$\lvert\lambda^{(ue)}\lambda^{(u\mu)}\rvert$	$\lesssim 4\cdot 10^{-4}$	$\mu^- \to e^- e^+ e^-$
$\lvert\lambda^{(ue)}_{V_3}\lambda^{(u\mu)}_{V_3}\rvert$	$\lesssim 2\cdot 10^{-4}$	
$\lvert\lambda^{(ce)}_{\tilde V_1,\tilde V_2}\lambda^{(c\mu)}_{\tilde V_1,\tilde V_2}\rvert$	$\lesssim 8\cdot 10^{-4}$	
$\lvert\lambda^{(ce)}_{V_2}\lambda^{(c\mu)}_{V_2}\rvert$	$\lesssim 6\cdot 10^{-4}$	
$\lvert\lambda^{(ce)}_{V_3}\lambda^{(c\mu)}_{V_3}\rvert$	$\lesssim 3\cdot 10^{-4}$	

TABLE XIV: Vector leptoquark constraints for real couplings scaling as TeV$/M$. For the constraint on $\tilde V_{1,2}$ from Q_w we apply its 2σ interval. For V_3 all constraints have to be multiplied with a factor of $1/2$.

couplings/mass	constraint	observable
$\lvert\lambda_{S_1L}^{(ul)}\lambda_{S_1L}^{(cl')}\rvert$	$\lesssim 4\cdot 10^{-4}$	$(K^+\to\pi^+\bar\nu\nu)/(K^+\to\pi^0\bar e\nu_e)$
$\lvert\lambda_{S_2R}^{(ue)}\lambda_{S_2R}^{(ce)}\rvert$	$\lesssim 2\cdot 10^{-3}$	$K_L^0\to\bar e e$
$\lvert\lambda_{S_2R}^{(u\mu)}\lambda_{S_2R}^{(ce)}\rvert$	$\lesssim 1\cdot 10^{-5}$	$K_L^0\to\bar e\mu$
$\lvert\lambda_{S_2R}^{(u\mu)}\lambda_{S_2R}^{(c\mu)}\rvert$	$\lesssim 3\cdot 10^{-4}$	$K_L^0\to\bar\mu\mu$
$\lvert\lambda_{S_3}^{(ue)}\lambda_{S_3}^{(ce)}\rvert$	$\lesssim 4\cdot 10^{-4}$	$(K^+\to\pi^+\bar\nu\nu)/(K^+\to\pi^0\bar e\nu_e)$
$\lvert\lambda_{S_3}^{(ue)}\lambda_{S_3}^{(c\mu)}\rvert,\quad\lvert\lambda_{S_3}^{(u\mu)}\lambda_{S_3}^{(ce)}\rvert$	$\lesssim 1\cdot 10^{-5}$	$K_L^0\to\bar e\mu$
$\lvert\lambda_{S_3}^{(u\mu)}\lambda_{S_3}^{(c\mu)}\rvert$	$\lesssim 3\cdot 10^{-4}$	$K_L^0\to\bar\mu\mu$
$\lvert\lambda_{V_2}^{(ue)}\lambda_{V_2}^{(ce)}\rvert$	$\lesssim 1\cdot 10^{-3}$	$K_L^0\to\bar e e$
$\lvert\lambda_{V_2}^{(ue)}\lambda_{V_2}^{(c\mu)}\rvert,\quad\lvert\lambda_{V_2}^{(u\mu)}\lambda_{V_2}^{(ce)}\rvert$	$\lesssim 5\cdot 10^{-6}$	$K_L^0\to\bar e\mu$
$\lvert\lambda_{V_2}^{(u\mu)}\lambda_{V_2}^{(c\mu)}\rvert$	$\lesssim 2\cdot 10^{-4}$	$K_L^0\to\bar\mu\mu$
$\lvert\lambda_{V_3}^{(ue)}\lambda_{V_3}^{(ce)}\rvert$	$\lesssim 8\cdot 10^{-5}$	$(K^+\to\pi^+\bar\nu\nu)/(K^+\to\pi^0\bar e\nu_e)$
$\lvert\lambda_{V_3}^{(ue)}\lambda_{V_3}^{(c\mu)}\rvert,\quad\lvert\lambda_{V_3}^{(u\mu)}\lambda_{V_3}^{(ce)}\rvert$	$\lesssim 3\cdot 10^{-6}$	$K_L^0\to\bar e\mu$
$\lvert\lambda_{V_3}^{(u\mu)}\lambda_{V_3}^{(c\mu)}\rvert$	$\lesssim 7\cdot 10^{-5}$	$K_L^0\to\bar\mu\mu$

TABLE XV: Constraints on the leptoquark coupling products from kaon decays [54] scaling as TeV$/M$.

where Z is the proton number and N is the neutron number, we find

$$\begin{aligned}
&\delta_{S_1}C_{1u}=\delta_{S_2}C_{1u}=-\frac{\sqrt{2}}{8G_F}\frac{\left|\lambda_R^{(ue)}\right|^2-\left|\lambda_L^{(ue)}\right|^2}{M^2}\,,\quad \delta_{S_2}C_{1d}=-\frac{\sqrt{2}}{8G_F}\frac{\left|\lambda_{S_2R}^{(ue)}\right|^2}{M^2}\,,\\
&\delta_{S_3}C_{1u}=\frac{1}{2}\delta_{S_3}C_{1d}=\frac{\sqrt{2}}{8G_F}\frac{\left|\lambda_{S_3}^{(ue)}\right|^2}{M^2}\,,\\
&\delta_{\tilde V_1}C_{1u}=\delta_{\tilde V_2}C_{1u}=\frac{\sqrt{2}}{4G_F}\frac{\left|\lambda_{\tilde V_{1,2}}^{(ue)}\right|^2}{M^2}\,,\\
&\delta_{V_3}C_{1u}=-\frac{\sqrt{2}}{2G_F}\frac{\left|\lambda_{V_3}^{(ue)}\right|^2}{M^2}\,,\quad \delta_{V_3}C_{1d}=-\frac{\sqrt{2}}{4G_F}\frac{\left|\lambda_{V_3}^{(ue)}\right|^2}{M^2}\,.
\end{aligned}\tag{F3}$$

We do not match V_2 due to an additional d_R-quark coupling [45].

The shift in the anomalous magnetic moment of a fermion f due to a scalar LQ reads [86]

$$\begin{aligned}
\Delta^S a_f=-\frac{3m_f}{16\pi^2}\frac{1}{M^2}\Bigg(&m_f\left(\left|\lambda_L^{(ff')}\right|^2+\left|\lambda_R^{(ff')}\right|^2\right)\left(\frac{1}{3}Q_e^{(f')}-\frac{1}{6}Q_e\right)\\
&+m_{f'}\mathrm{Re}\left[\lambda_L^{(ff')}\left(\lambda_R^{(ff')}\right)^*\right]\left(\left(-3-2\ln\frac{m_{f'}^2}{M^2}\right)Q_e^{(f')}-Q_e\right)\Bigg)
\end{aligned}\tag{F4}$$

($m_{f'}\to -m_{f'}$ and $\lambda\to\lambda^*$ for $S_{1,3}$). Here, Q_e and $Q_e^{(f')}$ denote the electric charges of the leptoquark and the fermion f' in the loop, respectively. The contribution to the electric dipole moment of f reads [86]

$$d_f=\frac{e}{32\pi^2}\frac{1}{M^2}m_{f'}\mathrm{Im}\left[\lambda_L^{(ff')}\left(\lambda_R^{(ff')}\right)^*\right]\left(\left(-3-2\ln\frac{m_{f'}^2}{M^2}\right)Q_e^{(f')}-Q_e\right)\,,\tag{F5}$$

times 3 for color if f' is a quark. For electrons $|d_e^{\mathrm{SM}}|\le 10^{-38}\,e$ cm [87]. The neutron electric dipole moment receives contributions from quarks $d_n=4/3d_d-1/3d_u$, with $d_n^{\mathrm{SM}}\sim\mathcal{O}(10^{-34})\,e$ cm [88].

The lepton flavor violating radiative muon decay in case of a scalar LQ is [89]

$$\delta_S\mathcal{B}_{\mu\to e\gamma}=\frac{\alpha_e}{4\Gamma_\mu}m_\mu^5\left(|F_{2LR}^\gamma|^2+|F_{2RL}^\gamma|^2\right)\,,\tag{F6}$$

where we note the typo $F_1 \leftrightarrow F_2$ in [89]

$$F^{\gamma}_{2LR,2RL} = \frac{3}{16\pi^2}\frac{1}{M^2}\left(\lambda^{(q\mu)}_{L,R}\left(\lambda^{(qe)}_{L,R}\right)^*\left(\frac{1}{6}Q^{(q)}_e - \frac{1}{12}Q_e\right)\right.$$
$$\left. - \frac{m_q}{m_\mu}\lambda^{(q\mu)}_{R,L}\left(\lambda^{(qe)}_{L,R}\right)^*\left(\left(-\frac{3}{2} - \ln\frac{m_q^2}{M^2}\right)Q^{(q)}_e - \frac{1}{2}Q_e\right)\right) \tag{F7}$$

($m_q \to -m_q$ and $\lambda \to \lambda^*$ for S_2). In case of a vector LQ [45]

$$\delta_V \mathcal{B}_{\mu\to e\gamma} = \frac{1}{\Gamma_\mu}\frac{m_\mu}{8\pi}\left(\left|F^V\right|^2 + \left|F^A\right|^2\right) \tag{F8}$$

with

$$\left|F^{V,A}\right| = \sqrt{\alpha_e 4\pi}\frac{\left|\lambda^{(qe)}\lambda^{(q\mu)}\right|}{32\pi^2}\frac{m_\mu^2}{M^2}\left(Q^{(q)}_e 2 + Q_e\frac{5}{2}\right) \tag{F9}$$

(times 2 for up-type quarks in scenario V_3).

The lepton flavor violating muon decay in case of a scalar LQ is [90]

$$\begin{aligned}
\delta_S \mathcal{B}_{\mu\to eee} = \frac{\alpha_e^2 m_\mu^5}{32\pi\Gamma_\mu}\Bigg(& |T_{1L}|^2 + |T_{1R}|^2 + \frac{2}{3}\left(|T_{2L}|^2 + |T_{2R}|^2\right)\left(8\ln\frac{m_\mu}{2m_e} - 11\right) \\
& - 4\mathrm{Re}[T_{1L}T^*_{2R} + T_{2L}T^*_{1R}] \\
& + \frac{1}{3}\left(2\left(|Z_L g_{Ll}|^2 + |Z_R g_{Rl}|^2\right) + |Z_L g_{Rl}|^2 + |Z_R g_{Ll}|^2\right) \\
& + \frac{1}{6}\left(|B_{1L}|^2 + |B_{1R}|^2\right) + \frac{1}{3}\left(|B_{2L}|^2 + |B_{2R}|^2\right) \\
& + \frac{2}{3}\mathrm{Re}[(T_{1L}B^*_{1L} + T_{1L}B^*_{2L} + T_{1R}B^*_{1R} + T_{1R}B^*_{2R}] \\
& - \frac{4}{3}\mathrm{Re}[T_{2R}B^*_{1L} + T_{2L}B^*_{1R} + T_{2L}B^*_{2R} + T_{2R}B^*_{2L}] \\
& + \frac{2}{3}\mathrm{Re}[B_{1L}Z^*_L g_{Ll} + B_{1R}Z^*_R g_{Rl} + B_{2L}Z^*_L g_{Rl} + B_{2R}Z^*_R g_{Ll}] \\
& + \frac{2}{3}\mathrm{Re}[2(T_{1L}Z^*_L g_{Ll} + T_{1R}Z^*_R g_{Rl}) + T_{1L}Z^*_L g_{Rl} + T_{1R}Z^*_R g_{Ll}] \\
& + \frac{2}{3}\mathrm{Re}[-4(T_{2R}Z^*_L g_{Ll} + T_{2L}Z^*_R g_{Rl}) - 2(T_{2L}Z^*_R g_{Ll} + T_{2R}Z^*_L g_{Rl})]\Bigg),
\end{aligned} \tag{F10}$$

where we correct the typo in $Z_{L,R}$ related terms in [90]

$$T_{1L,1R} = -\frac{3}{16\pi^2}\frac{1}{M^2}\lambda^{(q\mu)}_{L,R}\left(\lambda^{(qe)}_{L,R}\right)^*\left(\left(\frac{4}{9} + \frac{1}{3}\ln\frac{m_q^2}{M^2}\right)Q^{(q)}_e + \frac{-1}{18}Q_e\right), \tag{F11}$$

$$\begin{aligned}
T_{2L,2R} = \frac{3}{16\pi^2}\frac{1}{M^2}\Bigg(& -\left(\lambda^{(q\mu)}_{R,L}\left(\lambda^{(qe)}_{R,L}\right)^*\frac{1}{6} + \frac{m_q}{m_\mu}\lambda^{(q\mu)}_{R,L}\left(\lambda^{(qe)}_{L,R}\right)^*\left(-\frac{3}{2} - \ln\frac{m_q^2}{M^2}\right)\right)Q^{(q)}_e \\
& + \left(\lambda^{(q\mu)}_{R,L}\left(\lambda^{(qe)}_{R,L}\right)^*\frac{1}{12} + \frac{m_q}{m_\mu}\lambda^{(q\mu)}_{R,L}\left(\lambda^{(qe)}_{L,R}\right)^*\frac{1}{2}\right)Q_e\Bigg),
\end{aligned} \tag{F12}$$

$$\begin{aligned}
Z_{L,R} = & -\frac{3}{16\pi^2}\frac{1}{M^2}\lambda^{(q\mu)}_{L,R}\left(\lambda^{(qe)}_{L,R}\right)^*\frac{1}{m_Z^2\sin^2\theta_w\cos^2\theta_w} \\
& \times\left(m_\mu^2\frac{3}{8}2g_{Lq,Rq} - m_q^2\left(1 + \ln\frac{m_q^2}{M^2}\right)g_{Rq,Lq} + m_\mu^2\frac{3}{8}2(-g)\right),
\end{aligned} \tag{F13}$$

$$B_{1L,1R} = \frac{3}{32\pi^2}\lambda^{(q\mu)}_{L,R}\left(\lambda^{(qe)}_{L,R}\right)^*\left|\lambda^{(q'e)}_{L,R}\right|^2\frac{-1}{M^2}, \tag{F14}$$

$$B_{2L,2R} = \frac{3}{64\pi^2}\lambda^{(q\mu)}_{L,R}\left(\lambda^{(qe)}_{L,R}\right)^*\left|\lambda^{(q'e)}_{R,L}\right|^2\frac{-1}{M^2} \tag{F15}$$

and

$$g_{Lf,Rf} = T_3^{(f_L,f_R)} - Q_e^{(f)} \sin^2\theta_w \,, \quad g = T_3 - Q_e \sin^2\theta_w \tag{F16}$$

($m_q \to -m_q$, $\lambda \to \lambda^*$ and $g_L \leftrightarrow g_R$ for S_2). Here, T_3 is the third component of the weak isospin of the LQ and $f_{L,R}$ label chiral fermions, that is, $g_{Lf,Rf}$ are SM couplings and g is the LQ coupling. In case of a vector LQ [91]

$$\delta_V \mathcal{B}_{\mu\to eee} = \frac{3\alpha_e^2}{8\pi^2}\left(Q_e^{(q)}\right)^2 \ln^2 \frac{m_q^2}{M^2} \frac{\left|\lambda^{(q\mu)}\lambda^{(qe)}\right|^2}{G_F^2 M^4} \tag{F17}$$

(times 4 for up-type quarks in scenario V_3), where we neglect terms $\sim Q_e$, m_f^2/M^2-suppressed box-diagrams and m_f^2/m_Z^2-suppressed Z-diagrams.

Matching onto the $\mu - e$ conversion in nuclei rate [92]

$$\begin{aligned}\Gamma_{\mu-e} &= 4m_\mu^5 \left|\frac{1}{4}C_{DR}D + C_{SL}G_S^{(u,p)}S^{(p)} + C_{SL}G_S^{(u,n)}S^{(n)} + 2C_{VR}V^{(p)} + C_{VR}V^{(n)}\right|^2 \\ &+ 4m_\mu^5 \left|\frac{1}{4}C_{DL}D + C_{SR}G_S^{(u,p)}S^{(p)} + C_{SR}G_S^{(u,n)}S^{(n)} + 2C_{VL}V^{(p)} + C_{VL}V^{(n)}\right|^2\end{aligned} \tag{F18}$$

we find

$$\begin{aligned}
&\delta_S C_{VR} = -\frac{\lambda_R^{(ue)}\left(\lambda_R^{(u\mu)}\right)^*}{4M^2}\,, \quad \delta_S C_{VL} = -\frac{\lambda_L^{(ue)}\left(\lambda_L^{(u\mu)}\right)^*}{4M^2}\,, \\
&\delta_S C_{SR} = -\frac{\lambda_L^{(ue)}\left(\lambda_R^{(u\mu)}\right)^*}{4M^2}\,, \quad \delta_S C_{SL} = -\frac{\lambda_R^{(ue)}\left(\lambda_L^{(u\mu)}\right)^*}{4M^2}\,, \\
&\delta_S C_{DR,DL} = \frac{1}{2m_\mu}F^\gamma_{2RL,2LR}\,, \\
&\delta_{\tilde{V}_1} C_{VR} = \frac{\lambda_{\tilde{V}_1}^{(ue)}\left(\lambda_{\tilde{V}_1}^{(u\mu)}\right)^*}{2M^2}\,, \quad \delta_{V_2} C_{VR} = \frac{\lambda_{V_2}^{(u\mu)}\left(\lambda_{V_2}^{(ue)}\right)^*}{2M^2}\,, \\
&\delta_{\tilde{V}_2} C_{VL} = \frac{\lambda_{\tilde{V}_2}^{(u\mu)}\left(\lambda_{\tilde{V}_2}^{(ue)}\right)^*}{2M^2}\,, \quad \delta_{V_3} C_{VL} = \frac{\lambda_{V_3}^{(ue)}\left(\lambda_{V_3}^{(u\mu)}\right)^*}{M^2}\,, \\
&\delta_{\tilde{V}_1,V_2} C_{DR,DL} = -\frac{1}{4m_\mu^2\sqrt{\alpha_e 4\pi}}\left(\left|F^V\right| \pm \left|F^A\right|\right)\,, \\
&\delta_{\tilde{V}_2,V_3} C_{DR,DL} = -\frac{1}{4m_\mu^2\sqrt{\alpha_e 4\pi}}\left(\left|F^V\right| \mp \left|F^A\right|\right)
\end{aligned} \tag{F19}$$

($\lambda \to \lambda^*$ for S_2), where $F^\gamma_{2RL,2LR}$ are given by Eq. (F7) and $|F^{V,A}|$ are given by Eq. (F9) (times 2 for up-type quarks in scenario V_3). We neglect loop-suppressed gluonic interactions. The nucleon form factors are given as $G_S^{(u,p)} = 5.1$ and $G_S^{(u,n)} = 4.3$ [92] and we take the overlap integrals of muons and electrons weighted by proton and neutron densities for titanium and gold

$$\begin{aligned}
&D_{\mathrm{Ti}} = 0.0864\,, \quad S_{\mathrm{Ti}}^{(p)} = 0.0368\,, \quad S_{\mathrm{Ti}}^{(n)} = 0.0435\,, \quad V_{\mathrm{Ti}}^{(p)} = 0.0396\,, \quad V_{\mathrm{Ti}}^{(n)} = 0.0468\,, \\
&D_{\mathrm{Au}} = 0.189\,, \quad S_{\mathrm{Au}}^{(p)} = 0.0614\,, \quad S_{\mathrm{Au}}^{(n)} = 0.0918\,, \quad V_{\mathrm{Au}}^{(p)} = 0.0974\,, \quad V_{\mathrm{Au}}^{(n)} = 0.146\,.
\end{aligned} \tag{F20}$$

Matching onto the leptonic pseudoscalar decay rate [93]

$$\Gamma_{P\to l\nu} = \frac{G_F^2 f_P^2\left(m_P^2 - m_l^2\right)^2}{8\pi m_P^3}\left|m_l V_{qq'} + m_l\frac{\sqrt{2}}{4G_F}(C_{VRL} - C_{VLL}) + \frac{m_P^2}{m_q + m_{q'}}\frac{\sqrt{2}}{4G_F}(C_{SLR} - C_{SRR})\right|^2 \tag{F21}$$

we find

$$
\begin{aligned}
\delta_{S_1} C_{VLL} &= \frac{1}{2}\frac{\lambda^{(ql)}_{S_1 L}\left(\lambda^{(q'l)}_{S_1 L}\right)^*}{M^2}\,, \quad \delta_{S_1} C_{SRR} = -\frac{1}{2}\frac{\lambda^{(ql)}_{S_1 R}\left(\lambda^{(q'l)}_{S_1 L}\right)^*}{M^2}\,,\\
\delta_{S_2} C_{SRR} &= \frac{1}{2}\frac{\lambda^{(q'l)}_{S_2 R}\left(\lambda^{(ql)}_{S_2 L}\right)^*}{M^2}\,,\\
\delta_{S_3} C_{VLL} &= -\frac{1}{2}\frac{\lambda^{(ql)}_{S_3}\left(\lambda^{(q'l)}_{S_3}\right)^*}{M^2}\,,\\
\delta_{V_3} C_{VLL} &= -\frac{\lambda^{(q'l)}_{V_3}\left(\lambda^{(ql)}_{V_3}\right)^*}{M^2}\,,
\end{aligned}
\tag{F22}
$$

We do not match V_2 due to an additional d_L-quark coupling [45].

We deduce the shift in $R_{e/\mu} = \Gamma_{\pi\to e\nu_e}/\Gamma_{\pi\to\mu\nu_\mu}$

$$
\begin{aligned}
\delta_{LQ} R_{e/\mu} = R^{\mathrm{SM}}_{e/\mu}\frac{1}{\sqrt{2}G_F V_{ud}}\mathrm{Re}\Bigg[&\left(C^{(l=e)}_{VRL} - C^{(l=e)}_{VLL}\right) - \left(C^{(l=\mu)}_{VRL} - C^{(l=\mu)}_{VLL}\right)\\
&+ \frac{m_\pi^2}{m_u + m_d}\left(\frac{C^{(l=e)}_{SLR} - C^{(l=e)}_{SRR}}{m_e} - \frac{C^{(l=\mu)}_{SLR} - C^{(l=\mu)}_{SRR}}{m_\mu}\right)\Bigg]\,.
\end{aligned}
\tag{F23}
$$

and the shift in the CKM parameter

$$
\frac{\Delta^{LQ} V_{ud}}{V_{ud}} = \frac{\sqrt{2}}{4G_F} C^{(ue)}_{VLL}
\tag{F24}
$$

by means of quark beta decay normalized to muon decay.

We match onto nuclear beta decay parameters to constrain Wilson coefficients [94]

$$
-0.14\cdot 10^{-2} < \frac{G_F \alpha_e}{\sqrt{2}\pi}\frac{C_T + C_{T5}}{C_A} < 1.4\cdot 10^{-2} \quad (90\%\,\mathrm{C.L.})\,,
\tag{F25}
$$

where $C_A^{\mathrm{SM}} = -1.27\, G_F V_{ud}$.

We obtain no constraints better than $|\lambda| \lesssim M/\mathrm{TeV}$ from the decay $\pi^0 \to \mu e$, Δm_D via vector LQs [21], the $D^0 - \bar{D}^0$ lifetime difference [95, 96], the anomalous magnetic moment via vector LQs [97], the decay $Z \to ff$ via scalar LQs [98], the decay $Z \to e\mu$ via scalar LQs [89], triple correlation coefficients in nuclear beta decay [99–101] nor additional nuclear beta decay parameters [102].

---

[1] T. Blake, T. Gershon and G. Hiller, Ann. Rev. Nucl. Part. Sci. **65**, 8007 (2015) [arXiv:1501.03309 [hep-ex]].
[2] J. L. Hewett *et al.*, hep-ph/0503261.
[3] D. M. Asner *et al.*, Int. J. Mod. Phys. A **24**, S1 (2009) [arXiv:0809.1869 [hep-ex]].
[4] T. Aushev *et al.*, arXiv:1002.5012 [hep-ex].
[5] B. O'Leary *et al.* [SuperB Collaboration], arXiv:1008.1541 [hep-ex].
[6] I. Doršner, S. Fajfer, N. Košnik and I. Nišandžić, JHEP **1311**, 084 (2013) [arXiv:1306.6493 [hep-ph]].
[7] G. Hiller and M. Schmaltz, Phys. Rev. D **90**, no. 5, 054014 (2014) [arXiv:1408.1627 [hep-ph]].
[8] B. Gripaios, M. Nardecchia and S. A. Renner, JHEP **1505**, 006 (2015) [arXiv:1412.1791 [hep-ph]].
[9] L. Calibbi, A. Crivellin and T. Ota, arXiv:1506.02661 [hep-ph].
[10] M. Freytsis, Z. Ligeti and J. T. Ruderman, Phys. Rev. D **92**, no. 5, 054018 (2015) [arXiv:1506.08896 [hep-ph]].
[11] S. de Boer, B. Müller and D. Seidel, to appear, DO-TH 15/11, QFET-2015-27.
[12] C. Greub, T. Hurth, M. Misiak and D. Wyler, Phys. Lett. B **382**, 415 (1996) [hep-ph/9603417].
[13] S. Fajfer, P. Singer and J. Zupan, Eur. Phys. J. C **27**, 201 (2003) [hep-ph/0209250].
[14] K. G. Chetyrkin, M. Misiak and M. Munz, Phys. Lett. B **400**, 206 (1997) [Phys. Lett. B **425**, 414 (1998)] [hep-ph/9612313].
[15] C. Bobeth, M. Misiak and J. Urban, Nucl. Phys. B **574**, 291 (2000) [hep-ph/9910220].
[16] P. Gambino, M. Gorbahn and U. Haisch, Nucl. Phys. B **673**, 238 (2003) [hep-ph/0306079].
[17] M. Gorbahn and U. Haisch, Nucl. Phys. B **713**, 291 (2005) [hep-ph/0411071].
[18] G. Burdman, E. Golowich, J. L. Hewett and S. Pakvasa, Phys. Rev. D **66**, 014009 (2002) [hep-ph/0112235].

[19] A. Paul, I. I. Bigi and S. Recksiegel, Phys. Rev. D **83**, 114006 (2011) [arXiv:1101.6053 [hep-ph]].
[20] R. M. Wang, J. H. Sheng, J. Zhu, Y. Y. Fan and Y. G. Xu, Int. J. Mod. Phys. A **30**, no. 12, 1550063 (2015) [arXiv:1409.0181 [hep-ph]].
[21] T. Inami and C. S. Lim, Prog. Theor. Phys. **65**, 297 (1981) [Prog. Theor. Phys. **65**, 1772 (1981)].
[22] M. Czakon, U. Haisch and M. Misiak, JHEP **0703**, 008 (2007) [hep-ph/0612329].
[23] M. Gorbahn, U. Haisch and M. Misiak, Phys. Rev. Lett. **95**, 102004 (2005) [hep-ph/0504194].
[24] A. J. Buras and M. Munz, Phys. Rev. D **52**, 186 (1995) [hep-ph/9501281].
[25] C. Greub, V. Pilipp and C. Schupbach, JHEP **0812**, 040 (2008) [arXiv:0810.4077 [hep-ph]].
[26] Y. Amhis *et al.* [Heavy Flavor Averaging Group (HFAG) Collaboration], arXiv:1412.7515 [hep-ex].
[27] C. Bobeth, P. Gambino, M. Gorbahn and U. Haisch, JHEP **0404**, 071 (2004) doi:10.1088/1126-6708/2004/04/071 [hep-ph/0312090].
[28] T. Huber, E. Lunghi, M. Misiak and D. Wyler, Nucl. Phys. B **740**, 105 (2006) doi:10.1016/j.nuclphysb.2006.01.037 [hep-ph/0512066].
[29] S. Fajfer and S. Prelovsek, Phys. Rev. D **73**, 054026 (2006) [hep-ph/0511048].
[30] R. Aaij *et al.* [LHCb Collaboration], Phys. Lett. B **724**, 203 (2013) [arXiv:1304.6365 [hep-ex]].
[31] K. A. Olive *et al.* [Particle Data Group Collaboration], Chin. Phys. C **38**, 090001 (2014).
[32] L. G. Landsberg, Phys. Rept. **128**, 301 (1985).
[33] L. Cappiello, O. Cata and G. D'Ambrosio, JHEP **1304**, 135 (2013) [arXiv:1209.4235 [hep-ph]].
[34] C. Bobeth, G. Hiller and G. Piranishvili, JHEP **0712**, 040 (2007) [arXiv:0709.4174 [hep-ph]].
[35] S. Fajfer and N. Košnik, Phys. Rev. D **87**, no. 5, 054026 (2013) [arXiv:1208.0759 [hep-ph]].
[36] S. Fajfer, arXiv:1509.01997 [hep-ph].
[37] S. Fajfer, S. Prelovsek and P. Singer, Phys. Rev. D **64**, 114009 (2001) [hep-ph/0106333].
[38] S. Fajfer, N. Kosnik and S. Prelovsek, Phys. Rev. D **76**, 074010 (2007) [arXiv:0706.1133 [hep-ph]].
[39] C. Delaunay, J. F. Kamenik, G. Perez and L. Randall, JHEP **1301**, 027 (2013) [arXiv:1207.0474 [hep-ph]].
[40] A. Paul, A. De La Puente and I. I. Bigi, Phys. Rev. D **90**, no. 1, 014035 (2014) [arXiv:1212.4849 [hep-ph]].
[41] I. Dorsner, S. Fajfer and N. Kosnik, Phys. Rev. D **86**, 015013 (2012) [arXiv:1204.0674 [hep-ph]].
[42] W. Buchmuller, R. Ruckl and D. Wyler, Phys. Lett. B **191**, 442 (1987) [Phys. Lett. B **448**, 320 (1999)].
[43] S. Fajfer and N. Kosnik, Phys. Rev. D **79**, 017502 (2009) [arXiv:0810.4858 [hep-ph]].
[44] S. Davidson and S. Descotes-Genon, JHEP **1011**, 073 (2010) [arXiv:1009.1998 [hep-ph]].
[45] S. Davidson, D. C. Bailey and B. A. Campbell, Z. Phys. C **61**, 613 (1994) [hep-ph/9309310].
[46] A. M. Baldini *et al.*, arXiv:1301.7225 [physics.ins-det].
[47] Y. G. Cui *et al.* [COMET Collaboration], KEK-2009-10.
[48] L. Bartoszek *et al.* [Mu2e Collaboration], arXiv:1501.05241 [physics.ins-det].
[49] I. de Medeiros Varzielas and G. Hiller, JHEP **1506**, 072 (2015) [arXiv:1503.01084 [hep-ph]].
[50] I. de Medeiros Varzielas and G. G. Ross, Nucl. Phys. B **733**, 31 (2006) [hep-ph/0507176].
[51] G. Altarelli and F. Feruglio, Nucl. Phys. B **741**, 215 (2006) [hep-ph/0512103].
[52] C. D. Froggatt and H. B. Nielsen, Nucl. Phys. B **147**, 277 (1979).
[53] J. F. Kamenik and C. Smith, Phys. Lett. B **680**, 471 (2009) [arXiv:0908.1174 [hep-ph]].
[54] M. Carpentier and S. Davidson, Eur. Phys. J. C **70**, 1071 (2010) [arXiv:1008.0280 [hep-ph]].
[55] K. G. Chetyrkin, J. H. Kuhn and M. Steinhauser, Comput. Phys. Commun. **133**, 43 (2000) [hep-ph/0004189].
[56] S. Fajfer and N. Košnik, arXiv:1510.00965 [hep-ph].
[57] R. Aaij *et al.* [LHCb Collaboration], Phys. Lett. B **754**, 167 (2016) doi:10.1016/j.physletb.2016.01.029 [arXiv:1512.00322 [hep-ex]].
[58] M. Ablikim *et al.* [BESIII Collaboration], arXiv:1512.06998 [hep-ex].
[59] [UTfit Collaboration], `http://www.utfit.org/UTfit/`
[60] D. M. Asner *et al.* [CLEO Collaboration], Phys. Rev. D **81**, 052007 (2010) [arXiv:0912.4232 [hep-ex]].
[61] S. Aoki *et al.*, Eur. Phys. J. C **74**, 2890 (2014) [arXiv:1310.8555 [hep-lat]].
[62] N. Carrasco *et al.* [ETM Collaboration], Phys. Rev. D **92**, 034516 (2015) [arXiv:1505.06639 [hep-lat]].
[63] S. G. Porsev, K. Beloy and A. Derevianko, Phys. Rev. D **82**, 036008 (2010) [arXiv:1006.4193 [hep-ph]].
[64] V. A. Dzuba, J. C. Berengut, V. V. Flambaum and B. Roberts, Phys. Rev. Lett. **109**, 203003 (2012) [arXiv:1207.5864 [hep-ph]].
[65] V. Cirigliano and I. Rosell, Phys. Rev. Lett. **99**, 231801 (2007) [arXiv:0707.3439 [hep-ph]].
[66] T. Aoyama, M. Hayakawa, T. Kinoshita and M. Nio, Phys. Rev. D **91**, no. 3, 033006 (2015) [arXiv:1412.8284 [hep-ph]].
[67] T. Suzuki, D. F. Measday and J. P. Roalsvig, Phys. Rev. C **35**, 2212 (1987).
[68] C. Greub, T. Hurth and D. Wyler, Phys. Rev. D **54**, 3350 (1996) [hep-ph/9603404].
[69] N. Isgur and M. B. Wise, Phys. Rev. D **42**, 2388 (1990).
[70] J. Charles, A. Le Yaouanc, L. Oliver, O. Pene and J. C. Raynal, Phys. Rev. D **60**, 014001 (1999) [hep-ph/9812358].
[71] C. Bobeth, G. Hiller, D. van Dyk and C. Wacker, JHEP **1201**, 107 (2012) [arXiv:1111.2558 [hep-ph]].
[72] M. Beneke and T. Feldmann, Nucl. Phys. B **592**, 3 (2001) [hep-ph/0008255].
[73] J. Koponen, arXiv:1311.6931 [hep-lat].
[74] S. Fukae, C. S. Kim, T. Morozumi and T. Yoshikawa, Phys. Rev. D **59**, 074013 (1999) [hep-ph/9807254].
[75] A. Ghinculov, T. Hurth, G. Isidori and Y. P. Yao, Nucl. Phys. B **685**, 351 (2004) [hep-ph/0312128].
[76] I. R. Blokland, A. Czarnecki, M. Slusarczyk and F. Tkachov, Phys. Rev. D **71**, 054004 (2005) [Phys. Rev. D **79**, 019901 (2009)] [hep-ph/0503039].

[77] A. Pak and A. Czarnecki, Phys. Rev. D **78**, 114015 (2008) [arXiv:0808.3509 [hep-ph]].
[78] A. Ali, G. Hiller, L. T. Handoko and T. Morozumi, Phys. Rev. D **55**, 4105 (1997) [hep-ph/9609449].
[79] G. Buchalla and G. Isidori, Nucl. Phys. B **525**, 333 (1998) [hep-ph/9801456].
[80] G. Aad *et al.* [ATLAS Collaboration], arXiv:1508.04735 [hep-ex].
[81] [CMS Collaboration], CMS-PAS-EXO-12-042.
[82] J. P. Saha, B. Misra and A. Kundu, Phys. Rev. D **81**, 095011 (2010) [arXiv:1003.1384 [hep-ph]].
[83] E. Golowich and A. A. Petrov, Phys. Lett. B **625**, 53 (2005) [hep-ph/0506185].
[84] A. A. Petrov, arXiv:1312.5304 [hep-ph].
[85] M. I. Gresham, I. W. Kim, S. Tulin and K. M. Zurek, Phys. Rev. D **86**, 034029 (2012) [arXiv:1203.1320 [hep-ph]].
[86] K. m. Cheung, Phys. Rev. D **64**, 033001 (2001) [hep-ph/0102238].
[87] M. E. Pospelov and I. B. Khriplovich, Sov. J. Nucl. Phys. **53**, 638 (1991) [Yad. Fiz. **53**, 1030 (1991)].
[88] A. Czarnecki and B. Krause, Phys. Rev. Lett. **78**, 4339 (1997) [hep-ph/9704355].
[89] R. Benbrik and C. K. Chua, Phys. Rev. D **78**, 075025 (2008) [arXiv:0807.4240 [hep-ph]].
[90] R. Benbrik, M. Chabab and G. Faisel, arXiv:1009.3886 [hep-ph].
[91] A. A. Gvozdev, A. V. Kuznetsov, N. V. Mikheev and L. A. Vasilevskaya, Phys. Lett. B **345**, 490 (1995) [hep-ph/9411278].
[92] R. Kitano, M. Koike and Y. Okada, Phys. Rev. D **66**, 096002 (2002) [Phys. Rev. D **76**, 059902 (2007)] [hep-ph/0203110].
[93] J. Barranco, D. Delepine, V. Gonzalez Macias and L. Lopez-Lozano, arXiv:1404.0454 [hep-ph].
[94] F. Wauters, A. García and R. Hong, Phys. Rev. C **89**, no. 2, 025501 (2014) [Phys. Rev. C **91**, no. 4, 049904 (2015)] [arXiv:1306.2608 [nucl-ex]].
[95] J. S. Hagelin, Nucl. Phys. B **193**, 123 (1981).
[96] A. Dighe, A. Kundu and S. Nandi, Phys. Rev. D **76**, 054005 (2007) [arXiv:0705.4547 [hep-ph]].
[97] J. P. Leveille, Nucl. Phys. B **137**, 63 (1978).
[98] G. Bhattacharyya, J. R. Ellis and K. Sridhar, Phys. Lett. B **336**, 100 (1994) [Phys. Lett. B **338**, 522 (1994)] [hep-ph/9406354].
[99] T. E. Chupp *et al.*, Phys. Rev. C **86**, 035505 (2012) [arXiv:1205.6588 [nucl-ex]].
[100] A. Kozela *et al.*, Phys. Rev. Lett. **102**, 172301 (2009) [arXiv:0902.1415 [nucl-ex]].
[101] R. Huber *et al.*, Phys. Rev. Lett. **90**, 202301 (2003) [nucl-ex/0301010].
[102] E. G. Adelberger *et al.* [ISOLDE Collaboration], Phys. Rev. Lett. **83**, 1299 (1999) [Phys. Rev. Lett. **83**, 3101 (1999)] [nucl-ex/9903002].